





Review

Inflaming the Brain with Iron

Pamela J. Urrutia^{1,†}, Daniel A. Bórquez^{2,†}  and Marco Tulio Núñez^{1,*} 

¹ Department of Biology, Faculty of Sciences, Universidad de Chile, 7800024 Santiago, Chile; pamela.urrutia.v@gmail.com

² Center for Biomedical Research, Faculty of Medicine, Universidad Diego Portales, 8370007 Santiago, Chile; daniel.borquez@udp.cl

* Correspondence: mnunez@uchile.cl; Tel.: +56-2-29787360

† P.J. Urrutia and D.A. Bórquez contributed equally to this work as first authors.

Abstract: Iron accumulation and neuroinflammation are pathological conditions found in several neurodegenerative diseases, including Alzheimer's disease (AD) and Parkinson's disease (PD). Iron and inflammation are intertwined in a bidirectional relationship, where iron modifies the inflammatory phenotype of microglia and infiltrating macrophages, and in turn, these cells secrete diffusible mediators that reshape neuronal iron homeostasis and regulate iron entry into the brain. Secreted inflammatory mediators include cytokines and reactive oxygen/nitrogen species (ROS/RNS), notably hepcidin and nitric oxide ($\cdot\text{NO}$). Hepcidin is a small cationic peptide with a central role in regulating systemic iron homeostasis. Also present in the cerebrospinal fluid (CSF), hepcidin can reduce iron export from neurons and decreases iron entry through the blood–brain barrier (BBB) by binding to the iron exporter ferroportin 1 (Fpn1). Likewise, $\cdot\text{NO}$ selectively converts cytosolic aconitase (c-aconitase) into the iron regulatory protein 1 (IRP1), which regulates cellular iron homeostasis through its binding to iron response elements (IRE) located in the mRNAs of iron-related proteins. Nitric oxide-activated IRP1 can impair cellular iron homeostasis during neuroinflammation, triggering iron accumulation, especially in the mitochondria, leading to neuronal death. In this review, we will summarize findings that connect neuroinflammation and iron accumulation, which support their causal association in the neurodegenerative processes observed in AD and PD.

Keywords: neuroinflammation; iron; Alzheimer's disease; Parkinson's disease; hepcidin; nitric oxide; iron regulatory protein 1; oxidative stress



Citation: Urrutia, P.J.; Bórquez, D.A.; Núñez, M.T. Inflaming the Brain with Iron. *Antioxidants* **2021**, *10*, 61. <https://doi.org/10.3390/antiox10010061>

Received: 9 December 2020

Accepted: 31 December 2020

Published: 6 January 2021

Publisher's Note: MDPI stays neutral with regard to jurisdictional claims in published maps and institutional affiliations.



Copyright: © 2021 by the authors. Licensee MDPI, Basel, Switzerland. This article is an open access article distributed under the terms and conditions of the Creative Commons Attribution (CC BY) license (<https://creativecommons.org/licenses/by/4.0/>).

1. Introduction

Brain iron overload in neurodegeneration-prone areas and in neuroinflammation has been broadly recognized as a pathological hallmark of neurodegenerative diseases, such as Alzheimer's disease (AD) and Parkinson's disease (PD). Neuroinflammation refers to the inflammatory responses mediated by the innate immune system that take place in the central nervous system (CNS). Although it shares many features with peripheral inflammation, the coexistence of CNS specialized cell types, such as microglia, astrocytes, neurons, endothelial cells, and pericytes, confers unique characteristics to brain inflammation. Furthermore, the loss of integrity of the blood–brain barrier (BBB) found in neuroinflammatory conditions allows the infiltration of peripheral inflammatory cells, such as macrophages [1].

The initiation of the progressive inflammatory process in AD and PD can be traced to the neurodegeneration of noradrenergic (NA) neurons in the locus coeruleus (LC), which is the earliest and more severely affected area in PD (Braak stage 2), followed by dopaminergic neurons of substantia nigra (SN; Braak stage 3) and ultimately, by the neurodegeneration of hippocampal and cortical neurons (Braak stage 5) [2]. Interestingly, in the most recent Braak staging of AD, tau pathology is first observed in the LC, later spreading to the entorhinal cortex and finally to other neocortical regions [3–5], suggesting shared molecular mechanisms with PD [6].

The selective vulnerability of LC-NA neurons correlates with their higher production of reactive oxygen species (ROS) under physiological conditions, which is significantly potentiated by peripheral inflammation, resulting in mitochondrial damage. An elevated expression of neuronal NADPH oxidase (NOX), which catalyzes the production of the superoxide radical (O_2^-), plays an important role in the selective susceptibility of LC-NA neurons [7]. Interestingly, LC neurodegeneration can be triggered by an intraperitoneal lipopolysaccharide (LPS) injection [8], suggesting that a gut–brain axis may play a significant role in PD pathogenesis, probably associated with a “body-first” PD subtype [9].

In the brain, norepinephrine (NE) significantly contributes to the suppression of neuroinflammatory responses, by attenuating microglial surveillance and activation, reducing the secretion of proinflammatory factors, and decreasing phagocytic NOX2-mediated $\cdot O_2^-$ production [10–14]. Accordingly, the use of N-(2-chloroethyl)-N-ethyl-2-bromobenzylamine (DSP-4), which is a selective NE toxin, potentiates neuroinflammation induced by amyloid β ($A\beta$)_{1–42} aggregates [15] or bacterial endotoxin lipopolysaccharide (LPS) [16,17] and promotes AD and PD pathogenesis in several animal models [16,18–26].

Microglia/macrophage activation can be followed during the progression of neurodegeneration by non-invasive techniques, such as positron emission tomography (PET), using radiotracers specifically designed for targeting the mitochondrial translocator protein 18-kDa (TSPO), which is a protein highly expressed in activated microglia/macrophages. Microglial/macrophage activation has been observed using PET in monkeys injected with the mitochondrial complex I inhibitor 1-methyl-4-phenyl-1,2,3,6-tetrahydropyridine (MPTP), which is a toxin that selectively kills dopaminergic neurons [27,28], and in rats expressing human A53T mutated α -synuclein in SN [29,30] or injected with the highly oxidizable dopamine analog 6-hydroxydopamine (6-OHDA) [31,32]. Altered glial immune responses have also been observed in animal models of familial PD [33,34] and in transgenic mice expressing AD-associated mutant proteins [35,36]. An increase in TSPO binding has been consistently observed in studies with AD [37] and PD [38] patients. However, there are several concerns about potential artifacts in microglial TSPO PET imaging, including binding to multiple cell types, such as astrocytes and endothelial cells [39,40]; differential tracer affinity in TSPO Ala147Thr polymorphism carriers [41]; and other confounding factors [42,43]. Therefore, the conclusions of these studies should be interpreted with caution. Interestingly, a recent study on AD transgenic rats shows TSPO upregulation in astrocytes before microglia [44], urging the development of more specific tracers for studying the respective contributions of astrogliosis and microgliosis to the neurodegenerative process. Overall, the reported evidence points to a central role of neuroinflammation in the initiation and progression of neurodegenerative processes.

The activation of microglial cells triggers the release of diffusible mediators, including cytokines, ROS, and reactive nitrogen species (RNS). Remarkably, ROS/RNS generation is supported by two enzymatic systems: The NOX2 enzyme complex that synthesizes $\cdot O_2^-$, which, through its dismutation, generates hydrogen peroxide (H_2O_2), and the inducible form of nitric oxide synthase (iNOS), which generates $\cdot NO$. These enzymatic systems play a crucial role in AD- and PD-associated neurodegeneration, as revealed by the neuroprotection achieved by the pharmacological or genetic inhibition of NOX2 or iNOS reported in animal models of AD [45,46] and PD [47–50].

Clinical evidence from patients displaying chronic use of non-steroidal anti-inflammatory drugs (NSAID) shows a reduced risk for AD [51,52] and PD [53]. Based on these epidemiological observations and the beneficial effects of NSAID in AD animal models, several clinical trials have been conducted to assess their efficacy in AD and dementia. Unfortunately, these studies have shown no significant effects on the cognitive performance in AD patients, prompting improvement of the therapeutic window and the use of more selective inhibitors in future clinical trials (reviewed in [54]).

Recently, neuroinflammation has been associated with the alteration of iron homeostasis, and at the same time, iron dyshomeostasis has been shown to play a pivotal role in the neuroinflammatory phenotype. As a result, neuroinflammation and iron are entangled in

a circuit that amplifies ROS production, leading to neuronal death. An analysis of post-mortem tissue from PD patients shows significant elevations in the concentration of iron in the SN, where degenerating neuromelanin-bearing dopaminergic neurons reside [55,56]. Similarly, iron is concentrated in and around AD senile plaques [57,58], in Huntington's disease basal ganglia [59], and in the spinal cord of sporadic amyotrophic lateral sclerosis patients [60]. Due to its paramagnetic property, iron's content can be estimated in specific brain areas using magnetic resonance imaging (MRI), by measuring the R2* relaxation rate, phase changes in susceptibility-weighted imaging (SWI), or susceptibility values upon quantitative susceptibility mapping (QSM) [61] [62,63]. Neuromelanin-sensitive MRI has also been proposed as a diagnostic tool for PD [64]. Significant increases in iron levels are measured in vivo by iron-sensitive MRI, even in the early stages of AD and PD patients, showing a good correlation with the severity of their symptoms [63,65,66]. Patients with familial PD-associated mutations also display increased brain iron deposition by MRI, even in asymptomatic stages [67], suggesting that iron accumulation plays a role in the progression of the idiopathic and genetic forms of PD.

Iron overload is also associated with several animal models of AD and PD. Transgenic mice for Amyloid precursor protein/presenilin-1 (APP/PS1) [68–71] and 5xFAD [72] exhibit increased brain iron levels. Moreover, an injection of MPTP, rotenone, or 6-OHDA phenocopies many aspects of PD in rodents, including iron accumulation in the SN [73–75]. Supporting a causal role of iron accumulation in neurodegeneration, neonatal iron supplementation in mice triggers the progressive neurodegeneration of SN dopaminergic neurons, reduces striatal dopamine levels, and increases the responsiveness to MPTP insult [76]. Moreover, chronic oral administration of iron induces iron accumulation in specific brain regions, including the SN and caudate/putamen. Iron accumulation is associated with oxidative stress-related dopaminergic neuronal apoptosis in the SN and with motor and cognitive deficits [77]. Consequently, iron chelation prevents neuronal death in several animal models of AD and PD [78–82] and iron chelation has recently been introduced as a new therapeutic concept for the treatment of PD [83,84]. Nevertheless, the results on the use of iron chelation treatment demonstrate that it slows that disease progression [85]. Due to the multifactorial nature of the neurodegenerative process in PD, a single target treatment, such as the use of chelators, may not fully stop the neurodegenerative process. Accordingly, treatment with multifunctional compounds with an iron chelating capacity and aimed at reducing two or more of the pathological events associated with the progress of the disease (a “multi-target” approach) may be better suited for the treatment of PD [85,86].

Aging is the main risk factor for the development of sporadic forms of AD and PD, and both iron accumulation and neuroinflammation exhibit an age-synchronous increment in the brain. Iron levels and microglial and astrocytic numbers are positively correlated in aged mice basal ganglia [87] and iron-retentive microglia concurring with elevated iron levels and oxidative stress in aged non-human primates [88]. Interestingly, a genetic predisposition to neuroinflammation aggravates the striatal iron-related poor cognitive switching ability in aged humans [89], highlighting the intimate relationship between iron and neuroinflammation during aging (reviewed in [90]).

Correspondingly, in this review, we present a summary of the mechanisms that underlie the bidirectional relationship between iron and neuroinflammation and its relevance to AD and PD pathogenesis.

2. Iron Homeostasis in the CNS

Iron is an essential protein cofactor that performs a myriad of unique functions in the CNS, including ribosome assembly, DNA repair, mitochondrial energy production, metabolite catabolism, myelination, and neurotransmitter anabolism and catabolism [91]. In excess, however, iron is linked to cellular death, causing sustained cellular oxidative stress by the iron-mediated catalytic conversion of H₂O₂ and ·O₂[−] into toxic hydroxyl radicals as a result of Fenton and Haber–Weiss chemistry, respectively [92]. Accordingly, iron homeostasis must be tightly controlled.

Transferrin (Tf), which is a glycoprotein that possesses two high-affinity iron (III)-binding sites, is the primary iron transporter into the CNS and thus plays an essential role in cellular iron uptake. Following transferrin binding to its surface receptor, TfR1, the Tf-TfR1 complex is endocytosed through clathrin-dependent pathways into the early endosome, in which its low pH induces iron dissociation from Tf. The ferrireductase Steap2 reduces Fe^{3+} to Fe^{2+} , which is transported into the cytoplasm by the divalent metal transporter-1 (DMT1). The apoTf/TfR1 complex returns to the plasma membrane, where the neutral pH induces its dissociation [93,94].

In the cytoplasm, iron is incorporated into the cytosolic labile iron pool (cLIP), which is distributed to three destinations: (i) To mitochondria, for the synthesis of iron-sulfur (Fe-S) clusters and heme prosthetic groups; (ii) to the cytoplasmic iron storage protein ferritin (Fn); or (iii) back to the extracellular fluid through the iron exporter, Fpn1. Ferritin is a multimeric protein assembled by 24 subunits of H and L monomers in a variable ratio, depending on the cellular type. The H subunit contains ferroxidase activity, while the L subunit is responsible for iron turnover at the ferroxidase site and iron nucleation within the Fn core [95].

Iron delivery to the brain is tightly regulated at the level of the BBB [94], composed of tight junction-adhered endothelial cells that safeguard the free access of molecules to the brain. Iron transport across the BBB is mediated by three mechanisms. Overall, the mechanism of iron transport across the BBB involves two transmembrane steps: Iron uptake at the luminal membrane of the brain capillary endothelial cells, followed by iron efflux into the brain interstitium at the abluminal membrane. The predominant mechanism involves the transcellular transport of iron through Tf endocytosis, DMT1-mediated transport from the endosome lumen into the cytoplasm, and Fpn1-mediated extrusion at the abluminal membrane [96–98]. A second mechanism involves Tf/TfR1 complex transcytosis across the endothelial cell and the release of Tf into the parenchyma at the abluminal membrane [99]. A third mechanism is dependent on Fn, which is present in blood serum and cerebrospinal fluid (CSF) [100–102]. Serum Fn is mainly composed of L subunits with one or two H subunits [95]. Both in vitro and in vivo studies have shown the transport of Fn across the BBB, utilizing different receptors [103–105]. The Scara5 receptor recognizes L-Fn [106], while H-Fn binds to TfR1 [107].

Iron released by brain vascular endothelial cells is quickly captured by nearby astrocytes, which play a critical role in regulating brain iron absorption at the abluminal side. Astrocytes do not express TfR1; however, DMT1 expression is highly polarized in astrocytes, in which DMT1 is mainly found in the end-foot processes associated with the BBB [108]. Therefore, iron released by the endothelial cells is probably taken up by nearby astrocytes through DMT1 and distributed to the brain parenchyma through Fpn1 [109]. The concentration of iron in the CSF ranges between 0.2 and 1.1 μM , whereas the concentration of Tf is about 0.24 μM [110,111]. Therefore, CSF iron levels often exceed the binding capacity of Tf [112] and iron is incorporated by neurons and glia from two sources: Transferrin-bound iron (TBI), through the Tf-TfR1 system, and non-transferrin bound iron (NTBI), through DMT1 or other iron transporters.

3. Role of Hepcidin in Neurodegeneration

Complex living organisms have developed sophisticated mechanisms to finely coordinate iron homeostasis and avoid iron overload. There is systemic iron regulation, mediated by hepcidin, and cellular iron regulation, through the iron regulatory element/iron regulatory protein (IRE/IRP) system. Both regulatory mechanisms are intertwined in a bidirectional relationship with inflammatory mediators, as detailed in the following text.

The peptide hormone hepcidin, mainly secreted into the bloodstream by hepatocytes, is the principal regulator of systemic iron homeostasis. Hepcidin controls dietary iron absorption, iron recycling by macrophages, and iron release from hepatic stores through the regulation of iron transporter levels, generating a decrease of iron plasma levels [113]. In enterocytes, hepcidin induces the internalization and proteasomal degradation

of apical-side DMT1, limiting early dietary iron absorption [114,115]. In comparison, in reticulo-endothelial cells (splenic macrophages and Kupffer cells in the liver) and hepatocytes, hepcidin binds to the Fpn1 C-terminal domain in an iron-dependent way, inducing its endocytosis and subsequent Fpn1 lysosomal degradation, enhancing iron sequestration [113,116,117].

Hepcidin expression is regulated by plasma iron levels, inflammation, and erythropoiesis. Regulation by iron plasma levels involves multiple pathways by which hepatocytes sense the circulating iron status. One pathway involves the secretion of iron-induced bone morphogenic protein (BMP) by liver sinusoidal endothelial cells [118]. BMP6 and BMP2 bind to the BMP receptor, triggering the phosphorylation and activation of SMAD1/5/8, which, complexed with SMAD4, translocates to the nucleus to induce hepcidin transcription [119,120]. Hepatocytes also sense plasma iron levels through the interaction of HFE with TfR1 and TfR2. Under low iron conditions, HFE binds to TfR1. Under high iron conditions, the binding of Tf-Fe to TfR1 displaces HFE that then binds to TfR2. The HFE/TfR2 complex interacts with hemojuvelin (HJV), potentiating the BMP signaling pathway and hepcidin transcription [121,122]. The inflammatory cytokines IL6, IL1 β , and IL22 induce hepcidin expression in hepatocytes through activation of the STAT3 signaling pathway [123–125]. The BMP/SMAD pathway is also involved in the regulation of hepcidin transcription downstream of inflammatory stimuli [126].

Since iron is required for hemoglobin synthesis, hepcidin expression is suppressed during erythropoiesis. The main erythroid regulator of hepcidin is erythroferrone, which is synthesized and secreted by developing erythroid cells [127], reviewed in [128]. Erythroferrone acts on hepatocytes, suppressing the production of hepcidin through a mechanism that involves targeting of the SMAD1/5 signaling pathway [129].

Hepcidin expression has also been described in the CNS. Hepcidin mRNA has been detected in several brain regions, including the cortex, hippocampus, amygdala, thalamus, hypothalamus, olfactory bulb, mesencephalon, cerebellum, pons, and spinal cord [130–132]. In the human brain, hepcidin has been detected in endosomal structures in reactive astrocytes and epithelial cells of the choroid plexus, colocalizing with Fpn1 [133]. Interestingly, during aging, both hepcidin mRNA and protein levels increase in the cerebral cortex, hippocampus, striatum, and SN [131,134]. The hepcidin peptide is also localized in the endothelium of blood vessels, choroid plexus, and pericytes [135], suggesting that brain hepcidin originates from both in situ production and systemic production [135,136]. Cell culture experiments showed that hepcidin is produced by microglia and astrocytes, as well as by pericytes [137,138].

Resembling the regulation of dietary iron absorption in the duodenum, hepcidin acts at the BBB, reducing iron entry into the brain. Hepcidin knockout (KO) mice show strongly increased Fpn1 immunoreactivity at the abluminal side of vascular endothelial cells [139], suggesting a reduction in Fpn1 turnover. At the BBB, hepcidin is secreted in a synaptic-like manner by astrocytes and only stimulates Fpn1 internalization and degradation in vascular endothelial cells in close proximity to astrocytes' end-feet, reducing iron export [104,140,141].

Hepcidin expression in the brain is regulated by inflammatory stimuli; for example, LPS and turpentine oil induce hepcidin expression in the cortex, hippocampus, and striatum [142–144]. Peripheral LPS administration also increases hepcidin mRNA and protein levels in the cerebral cortex, SN [145], and choroid plexus [146]. However, more studies are required to determine the contribution of peripheral inflammation upon brain iron homeostasis. Interestingly, the hepcidin expression in astrocytes is mainly dependent on the IL6-STAT3 pathway, since LPS treatment of IL6 null-derived primary cultures fails to induce an increase of hepcidin mRNA levels, in contrast with a robust induction in wild-type cultured cells [147]. The proposed mechanism involves LPS-mediated IL6 secretion from microglia, and the subsequent IL6-triggered hepcidin production in astrocytes by means of a STAT3-mediated pathway [148]. In astrocytes, hepcidin knockdown reduces the neuronal

iron accumulation, oxidative stress, and apoptosis generated by an LPS intraventricular injection [148], suggesting a deleterious role of hepcidin in neuroinflammation.

Understanding the function of hepcidin in the CNS is an ongoing process. Hepcidin can prevent iron accumulation in the brain, by inhibiting TfR1, DMT1, and Fpn1 expression on microvascular endothelial cells and thus reducing TBI and NTBI uptake [149]. However, several studies show conflicting results regarding the role of hepcidin in several neuronal pathologies. These discrepancies can partially be explained by the use of isolated cell cultures, which do not take into account the interaction between neurons and glial cells observed in the intact brain. Accordingly, hepcidin loss-of-function protects N27 rat dopaminergic cells from 6-OHDA-induced apoptosis, decreasing the intracellular iron content and oxidative stress [150]. In contrast, in vivo hepcidin overexpression in astrocytes prevents the increase in brain iron levels and oxidative stress in a systemic iron overload rat model [151] and reduces dopamine neuronal loss and limits iron accumulation in the SN in rotenone and 6-OHDA animal models of PD. Remarkably, hepcidin overexpression also promotes α -synuclein clearance through autophagy, reduces mitochondrial dysfunction, and improves motor deficits [152,153].

A protective role for hepcidin has also been reported in AD models. Hepcidin pretreatment reduces the secretion of inflammatory cytokines induced by the A β peptide and decreases the toxicity of astrocytes and microglia conditioned media in hippocampal neurons [154]. Moreover, hepcidin pretreatment reduces both the oxidative damage and the glial activation in the hippocampus displayed by animals after an intraventricular injection of A β [154]. Accordingly, in APP/PS1 transgenic mice, hepcidin overexpression by astrocytes reduces iron entry into the brain and diminishes iron accumulation in neurons, which results in decreased neuronal death in the cortex and hippocampus [155]. Interestingly, one study shows that hepcidin and Fpn1 are reduced in post-mortem tissue from AD patients [156], suggesting a key role of hepcidin in the development of this disease.

Overall, these findings suggest that hepcidin secretion by astrocytes exerts a spatially restricted action on endothelial cells, reducing iron entry into the brain and providing neuroprotection. On the other hand, under neuroinflammation, unleashed hepcidin expression triggered by IL6 can generate iron accumulation in neurons, promoting neurodegeneration.

4. Neuroinflammation Modulates the IRE/IRP System in Neurodegeneration

Changes in the cell iron status (iron overload or depletion) lead to compensating translational changes in the levels of iron homeostasis-related proteins through the iron regulatory element/iron regulatory protein (IRE/IRP) system. Inflammatory mediators (especially \cdot NO) can target the IRE/IRP system, completely reshaping iron homeostasis in neurons and glial cells and amplifying the neurotoxic effects of unresolved neuroinflammation. Two IRP isoforms, known as IRP1 and IRP2, modulate the expression of proteins by binding to conserved stem-loop structures, named IREs, in the untranslated regions (UTRs) of their mRNAs. The regulatory outcome depends on the position and context of the IRE in the mRNA sequence: IRP binding to the 5' UTR IRE region represses translation, whereas IRP binding to the 3' UTR IRE region indirectly stimulates translation through the suppression of mRNA degradation [157]. In iron-deficient cells, IRPs selectively bind IRE at the 5' UTR region of the mRNA coding for Fn and Fpn1 and to 3' UTR of the mRNA coding for TfR1 and DMT1, promoting iron uptake. In conditions of iron excess, IRP2 is degraded and the IRP1 apoprotein binds to a [4Fe-4S] cluster to convert it into cytosolic (c)-aconitase, suppressing its RNA-binding activity [158,159]. Diminished IRP binding to the IREs promotes Fn and Fpn1 synthesis, whereas the TfR1 and DMT1 mRNAs are degraded by nucleases.

As mentioned above, IRP1 is a bifunctional cytoplasmic protein that transits reversibly between two conformations: An active RNA-binding protein (properly IRP1) and a [4Fe-4S] cluster-bearing protein, inactive for RNA binding that functions as a c-aconitase. The c-aconitase has an exclusively dedicated maturation system by the cytosolic Fe-S cluster protein assembly (CIA) machinery, where the heterotrimeric complex (CIA2A)₂CIAO1

transfers one [4Fe-4S] cluster to IRP1, generating the active c-aconitase [160,161]. The CIA system depends on the mitochondrial Fe-S cluster assembly machinery (ISC). Therefore, IRP1 accumulates under iron deficiency conditions, when the ISC assembly machinery is impaired, acting as a sensor for the availability of mitochondrial iron and ensuring an adequate iron supply to this organelle [162,163].

Increased IRP1 IRE-binding activity has been observed in cells deficient in glutaredoxin 2 (GLRX2) [164], glutaredoxin 5 (GLRX5) [165], sideroflexin 4 (SFXN4) [166], or frataxin (FXN) [162], all of which are essential proteins for Fe-S cluster assembly. As IRP1 directs iron flux preferentially to the mitochondria, its unphysiological activation generates mitochondrial iron overload, and a deficiency in the availability of iron in the cytoplasm, which further potentiates iron entry into the cell through increases in TfR1 and diminished Fn levels [164–166].

Recently, an IRP1-dependent mitophagy activation mechanism has been described, suggesting that IRP1 could control mitochondrial iron recycling, analogous to the recycling of amino acids through macroautophagy. Mitophagy activation involves IRP1 binding to the 5' UTR IRE sequence on Bcl-xL mRNA, repressing its translation in cells under iron depletion or impaired Fe-S cluster biogenesis [167]. This mechanism is consistent with early observations showing that deferiprone, which is an iron chelator, specifically activates mitophagy rather than macroautophagy [168].

Through the regulation of erythroid-specific aminolevulinic acid synthase 2 (ALAS2), IRP1 also balances iron availability and its utilization by mitochondria. ALAS2 catalyzes the first step of heme biosynthesis and is negatively regulated by IRP1 binding to the 5' IRE sequence in ALAS2 mRNA. Under mitochondrial iron-deficient conditions induced by mitoferrin-1 deficiency, IRP1 activation and subsequent ALAS2 translation inhibition prevent the accumulation of protoporphyrin, which are the precursors of the heme group [169]. Heme binding also inhibits IRPs, since the heme concentration is expected to increase under mitochondrial iron sufficiency conditions. Heme binding decreases IRP activity by steric competence with IREs or by oxidatively-mediated degradation [170,171]. These IRP1 regulatory mechanisms and associated effectors are summarized in Figure 1.

Both IRP1 and IRP2 mostly share their target mRNAs, but IRP2 is activated through a different mechanism when compared to IRP1. Under iron sufficient conditions, IRP2 is constitutively degraded by the proteasome. The E3 ubiquitin ligase FBXL5 controls IRP2 polyubiquitination. In turn, FBXL5 is also regulated by the ubiquitin-proteasome system. The FBXL5 ligase has an N-terminal hemerythrin-like domain with a di-iron center, which allows its correct folding and provides protection against degradation [172–174]. Under iron deficiency conditions, the N-terminal domain partially unfolds and is polyubiquitinated by the HERC2 ubiquitin ligase [175]; FBXL5 also has a redox-sensitive [2Fe-2S] cluster in the C-terminal substrate recognition domain, which, upon oxidation, promotes IRP2 binding in an oxygen-dependent manner [176]. The CIA targeting complexes CIAO1, CIAO2B, and MMS19 exhibit an oxygen-dependent interaction with the C-terminal of FBXL5, potentiating IRP2 degradation [177]. These findings strongly suggest that these complexes could transfer the [2Fe-2S] cluster to FBXL5.

IRP1 KO mice show an apparently normal phenotype with tissue-specific iron dysregulation in brown fat and kidneys. Increased HIF2 α translation in the kidney of IRP1 KO juvenile animals leads to increased erythropoietin expression, splenomegaly, and polycythemia, although this phenotype is normalized in adult animals [178,179]. The HIF2 α mRNA contains a 5' IRE sequence preferentially recognized by IRP1, which would explain the selective effect on the IRP1-null background. In contrast, IRP2 KO mice exhibit the misregulation of iron homeostasis in several tissues, including the brain, duodenum, and bone marrow, which IRP1 fails to compensate for [180,181]. Accordingly, FBXL5-null mice die during embryonic development because of iron overload and oxidative stress, although the deletion of IRP2, but not IRP1, restores the viability [182,183].

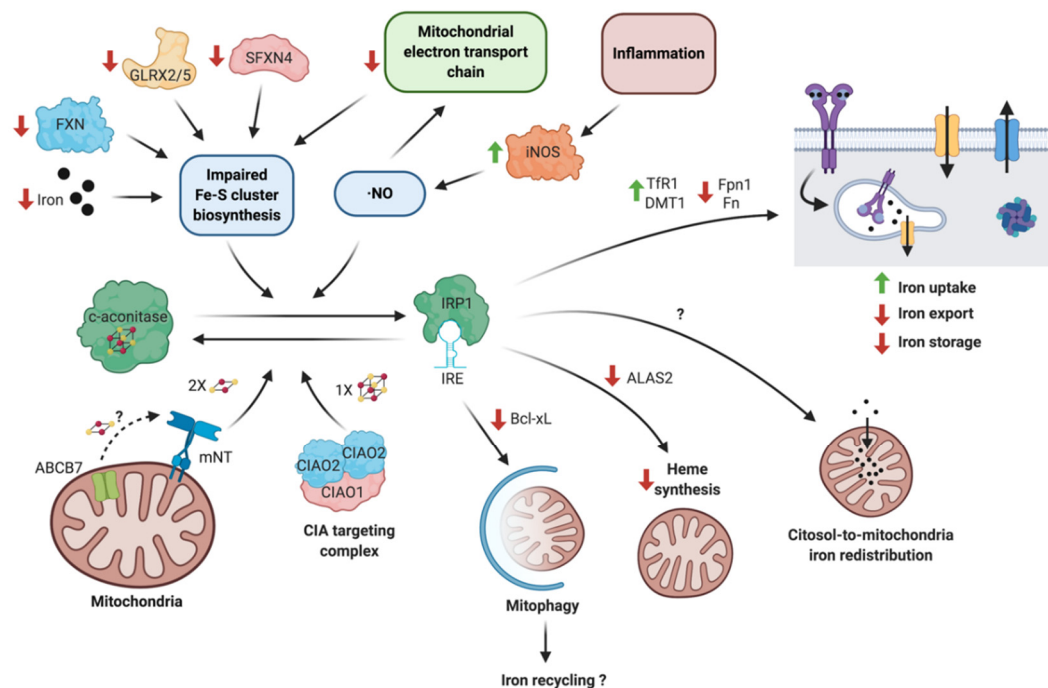


Figure 1. Regulatory mechanisms and functions of iron regulatory protein 1 (IRP1). The bifunctional protein c-aconitase/IRP1 is regulated by several mechanisms. C-aconitase is converted to IRP1 through two main processes: (i) Impaired Fe-S cluster biosynthesis, as a result of decreased mitochondrial iron availability, defects in the Fe-S cluster assembly (ISC) machinery, or bioenergetic failure, or (ii), through downstream inflammation by $\cdot\text{NO}$ -mediated Fe-S cluster disruption. Conversely, IRP1 is turned back into c-aconitase by mNT under oxidative stress or by a specialized branch of the CIA targeting complex. The binding of IRP1 to iron response elements (IRE) in specific mRNA targets regulates mitophagy, heme synthesis, iron redistribution to mitochondria, and iron uptake and storage. FXN: frataxin; GLRX2/5; Glutaredoxin-2/5; SFXN4: Sideroflexin 4; CIA: cytoplasmic iron-sulfur assembly; and mNT: mitoNEET. Created with BioRender.com.

In tissues, IRP1 is mainly found as c-aconitase and has a limited contribution to the control of iron homeostasis under physiological conditions, not significantly responding to iron starvation [181]. Interestingly, IRP1 is a poor iron sensor at low (tissular) oxygen tension, but it becomes relevant at 21% oxygen (cell culture conditions), suggesting that oxygen-derived reactive species are key to IRP1 activation [184]. For example, tempol, which is a nitroxide radical, can activate the large latent reservoir of IRE-binding activity in the form of c-aconitase, restoring iron homeostasis in an IRP2-null background [185].

In summary, IRP1 acts as a sensor for mitochondrial iron deficiency, activating mitophagy to recycle the iron contained in this organelle, and stimulating iron uptake to restore mitochondrial iron homeostasis, whereas IRP2 outcompetes IRP1 in the regulation of cellular iron homeostasis in physiological conditions. Inflammatory mediators such as ROS/RNS can trigger decomposition of the [4Fe-4S] cluster of c-aconitase, activating IRP1, even under iron sufficiency conditions. This paradoxical activation plays an important role in neurodegenerative processes. An intricate scenario is generated by inflammatory cell activation, which produces a diverse repertoire of ROS/RNS. In addition to $\cdot\text{O}_2^-$, H_2O_2 , and $\cdot\text{NO}$ produced by enzymatic systems, the highly reactive peroxynitrite and hydroxyl radical generated non-enzymatically also form part of this repertoire. Due to their differential reactivity and diffusibility, each ROS/RNS affects the Fe-S cluster of c-aconitase in a different way.

The superoxide anion attacks the c-aconitase, leading to Fe-S cluster loss and IRP1 activation. Cytosolic superoxide dismutase (SOD1) (but not mitochondrial SOD2) confers selective protection to c-aconitase, suggesting that $\cdot\text{O}_2^-$ action is limited to its compartment of origin [186]. Moreover, the $\cdot\text{O}_2^-$ -dependent intracellular oxidative stress observed in

SOD1-null mice drastically reduces IRP1 protein levels [187,188]. This adaptive regulation can be facilitated by FBXL5-mediated IRP1 degradation, thus preventing excessive IRE-binding activity [189]. Hence, under inflammatory conditions, $\cdot\text{O}_2^-$ is generated extracellularly and does not activate IRP1 [190].

In vitro, H_2O_2 converts purified c-aconitase into the [3Fe-4S] form, losing its aconitase activity, without eliciting IRE-binding activity [191]. Accordingly, only extracellular H_2O_2 (and not intracellular H_2O_2) triggers the conversion of c-aconitase into active IRP1 [190,192], indicating that H_2O_2 acts indirectly. Experiments performed on permeabilized cells show that the conversion of c-aconitase to IRP1 triggered by H_2O_2 requires membrane-associated components [193], strongly suggesting the participation of a signaling-mediated event [194]. The consequences of extracellular H_2O_2 treatment on human neuroblastoma cells, including Fpn1 degradation, IRP1-mediated H-Fn protein level reduction, and increased cLIP have been described [195].

The most important direct activator of the IRE-binding activity of IRP1 is $\cdot\text{NO}$, acting as the main transducer of $\cdot\text{NO}$ on iron metabolism. Nitric oxide triggers the conversion of c-aconitase to IRP1 through a disassembly of its [4Fe-4S] cluster [196–198], and therefore, it has no effect on IRP2 activity [199,200]. However, $\cdot\text{NO}$ only prompts the priming of apo-IRP1 for IRE binding; thioredoxin-mediated reduction of apo-IRP1 is needed for full RNA-binding activity [201]. Nitric oxide-mediated IRP1 activation increases TfR1 levels. Nitric oxide also activates H-Fn, L-Fn, and Fpn1 transcription, but parallel IRP1 activation represses its translation, resulting in largely preserved protein levels. Nitric oxide also induces Fe-S cluster disruption of mitochondrial (m)-aconitase, and IRP1 activation is essential for [4Fe-4S] cluster reconstitution, reinforcing its important role in mitochondrial iron sufficiency [200]. Finally, peroxynitrite disrupts the Fe-S cluster on c-aconitase and additionally induces tyrosine nitration of IRP1, inhibiting both aconitase and IRE-binding activity [196,197,202,203].

Upon oxidative disruption of the [4Fe-4S] cluster, IRP1 is quickly turned back into c-aconitase through a protein synthesis-independent mechanism [204]. This recycling pathway is mediated by mitoNEET (mNT), which is a dimeric [2Fe-2S] cluster-bearing protein located in the outer mitochondrial membrane. The mNT Fe-S cluster is resistant to H_2O_2 and $\cdot\text{NO}$ -mediated decomposition and each monomer successively transfers its cluster to reconstitute c-aconitase [205]. Interestingly, only the oxidized state of the mNT Fe-S cluster is competent for transfer [206]. Remarkably, mNT KO mice exhibit iron accumulation, mitochondrial dysfunction, decreased striatal tyrosine hydroxylase (TH), and dopamine levels and motor deficits, representing many of the characteristics of early neurodegeneration in PD [207], underlining the importance of this pathway in avoiding the hyper activation of IRP1 under oxidative stress.

The paradoxical activation of IRP1 despite elevated iron levels has been observed under inflammatory conditions and/or under unrestricted ROS/RNS production, leading to a positive feedback loop that generates iron overload and cell death [208,209]. For example, rotenone boosts ROS production through mitochondrial complex I inhibition, increases TfR1 and DMT1 and decreases Fpn1 protein levels, and enlarges the cLIP in an IRP1-dependent manner. Accordingly, IRP1 silencing abolishes the rotenone-induced iron uptake increase and reduces complex I inhibition-triggered neuronal death [210].

Inflammatory cytokines can enhance iron accumulation by regulating IRP1 activity through $\cdot\text{NO}$ -dependent and $\cdot\text{NO}$ -independent mechanisms [211]. In rat hepatoma cells, treatment with interferon (IFN)- γ /tumor necrosis factor (TNF)- α /LPS triggers $\cdot\text{NO}$ -mediated IRP1 activation without changes in IRP2, accompanied by the translational repression of Fn expression [199]. Similarly, in primary cultured hippocampal neurons, the pro-inflammatory cytokines TNF α and IL6 and the Toll-like receptor (TLR)-4 agonist LPS directly upregulate both the mRNA and protein levels of DMT1 and induce a transient decrease in Fpn1 protein levels, generating an increment of the iron content in neurons [137,212], which could be associated with IRP1 activation. Moreover, in primary cultures of ventral mesencephalic neurons, the pro-inflammatory cytokines IL1 β and TNF α

also promote iron influx and decrease iron efflux. Consistently, TfR1 and DMT1 (+IRE) are upregulated and Fpn1 is downregulated. These changes are mediated by the $\cdot\text{NO}$ - and ROS-mediated activation of IRP1, downstream of pro-inflammatory cytokines [213].

In vivo evidence also supports the role of paradoxical IRP1 activation in neurodegenerative diseases. Early findings showed that sustained IRP1 activity in PD can repress Fn translation, despite increased iron levels [214]. Similarly, IRP1 forms a more stable complex with IREs in AD brains, which could explain the absence of Fn upregulation [215]. The unexpected finding of an IRE sequence selectively recognized by IRP1 in the 5' UTR of APP mRNA generated a link between iron accumulation and A β deposition [216,217]. Additionally, IL1 β stimulates IRP1 binding to APP mRNA IRE, suggesting that inflammatory stimuli can decrease APP translation [216]. Two putative mechanisms have been proposed to explain the link between APP and iron homeostasis: APP interaction with Fpn1, in order to provide the necessary ferroxidase activity for the oxidation and transfer of the exported iron to Tf [218], and APP-mediated membrane Fpn1 stabilization [219–221]. Moreover, recent findings strongly suggest that $\cdot\text{NO}$ -mediated IRP1 activation diminishes APP levels and iron export in PD, promoting iron deposition [222]. In summary, ROS/RNS produced during inflammatory oxidative bursts can activate IRP1, promoting iron overload and neuronal death. Likewise, this mechanism has consequences on the inflammatory cells themselves, as addressed below.

5. Iron and Microglia/Macrophage M1/M2 Polarization

Macrophages and microglia play crucial roles in homeostatic and immune defense in the CNS. Upon infection or tissue injury, resident microglia are activated and peripheral macrophages are recruited to the CNS to eliminate pathogens or damaged cells. Additionally, microglia and macrophages have an anti-inflammatory or “resolving” function associated with tissue repair. Although tissular macrophages/microglia possess a broad spectrum of phenotypes, a simple bi-state model of inflammatory/classical (M1)- and resolution/alternative (M2)-activated macrophages/microglia has been widely used [223]. As described later in the text, M1 and M2 macrophages/microglia exhibit different iron homeostasis settings and their own differentiation is influenced by this metal ion.

The M1 phenotype can be induced by LPS and IFN γ treatment and is characterized by increased iNOS expression and the secretion of inflammatory cytokines such as IL6, IL1 β , and TNF α . On the other hand, M2 phenotype differentiation can be achieved by IL4 treatment and is characterized by increased arginase-1 levels and secretion of the brain-derived neurotrophic factor (BDNF), anti-inflammatory cytokines such as IL10, and several lipid mediators [223]. Interestingly, M1/M2 macrophages possess a completely opposite phenotype of iron handling (Figure 2). While M1 macrophages have lower IRP binding activity, low cLIP, lower levels of TfR1 and Fpn1, and higher levels of H-Fn, M2 macrophages have higher IRP binding activity, a larger cLIP, higher TfR1 and Fpn1 levels, and lower H-Fn levels. Functionally, M1 macrophages are less efficient in iron uptake and release and have a more limited response to extracellular iron deficiency or excess than M2 macrophages [224].

The homeostatic iron state of the M1 phenotype is achieved through regulation of the IRE/IRP system. Treatment of murine macrophages with IFN γ and LPS (to promote the M1 phenotype) induces a differential response upon the activities of IRP1 and IRP2 [225]. Treatment with IFN γ /LPS quickly activates IRP1 in an $\cdot\text{NO}$ -dependent manner, and triggers progressive, iron-dependent, IRP2 down regulation [226]. The iron homeostatic response is predominantly mediated by this IRP2 down regulation, since a translational derepression of Fn and an increase in its protein levels are observed; additionally, Tf/TfR1-mediated iron uptake is diminished [227–230]. The activation of NOX is presumably involved in the decrease in TfR1 expression mediated by LPS [231]. Overall, these studies are consistent with the observation that the microglial M1 phenotype supports iron incorporation through DMT1 and the M2 phenotype via the Tf-TfR1 system [232]. Although it is expected that TfR1 and DMT1 have the same expression pattern, since they both have IREs in the 5' UTR

region of their mRNAs, DMT1 is also stimulated at the transcriptional level by LPS/IFN γ in M1 macrophages, which would explain the antagonistic behavior of DMT1 and TfR1 regulation [233]. Additionally, LPS-treated macrophages reduce Fpn1 expression in an IRP- and \cdot NO-dependent manner [234]. The rapid IRP1 activation is followed by a decrease, also mediated by \cdot NO, of c-aconitase/IRP1 mRNA and protein levels [235], configuring the final iron phenotype of M1 macrophages described above.

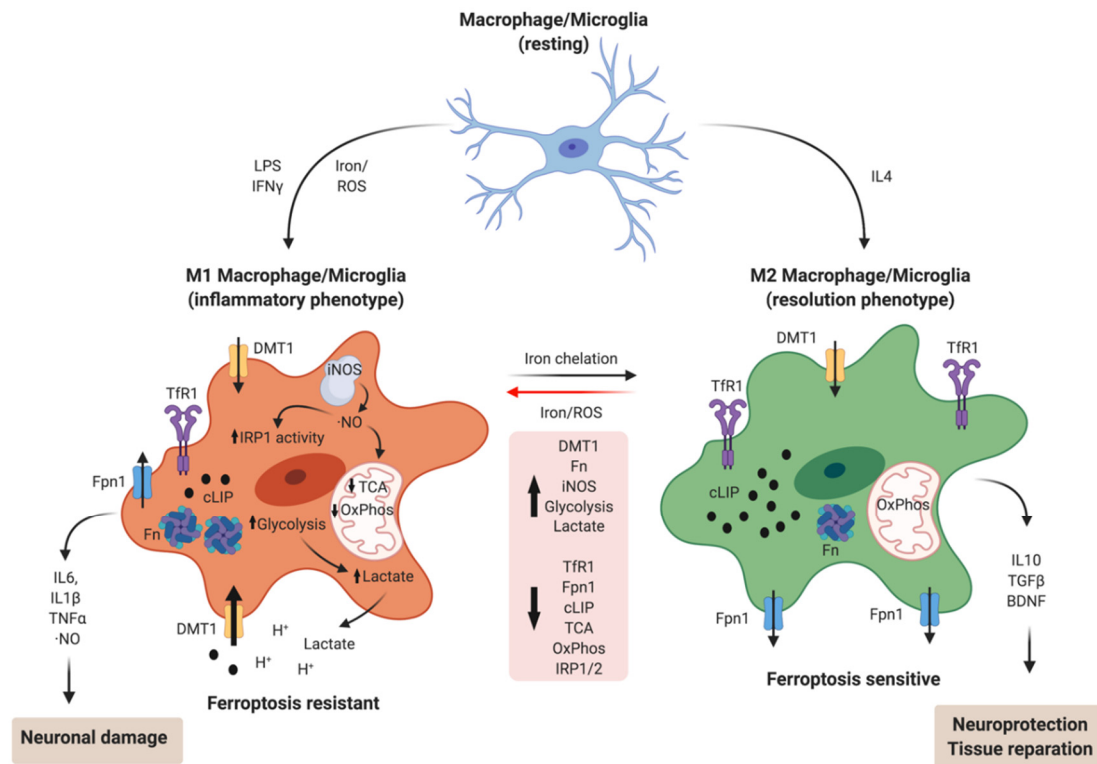


Figure 2. Iron homeostasis during macrophage/microglia M1/M2 polarization. Iron plays a central role in the balance between M1 inflammatory and M2 resolving phenotypes, stimulating M1 differentiation or converting the M2 phenotype into M1. In addition, \cdot NO generated by M1 macrophages/microglia reshapes cellular iron homeostasis, diminishing the cytosolic labile iron pool (cLIP) and reducing mitochondrial oxidative metabolism, thus conferring resistance to ferroptosis. Conversely, the M2 phenotype is ferroptosis-prone because of higher cLIP, energy dependence on oxidative phosphorylation, and the production of lipid oxidation products. Created with BioRender.com.

Additionally, iron modulates differentiation towards one or the other phenotype. Iron overload triggers M1 polarization via an ROS-mediated mechanism [236], increasing TNF α and IL1 β secretion [213] and causes M2 macrophages to switch their phenotype to M1 [237]. Accordingly, iron chelation with deferoxamine reduces RNS/ROS release and TNF α and IL1 β secretion by microglia [238] and also promotes microglial M2 polarization in APP/PS1 transgenic mice, together with reduced brain iron and A β _{1–42} deposition [239]. The brain-permeable iron chelator VK-28 also stimulates microglial polarization towards an M2-like phenotype [240]. Remarkably, the conditional deletion of H-Fn in macrophages reduces LPS/IFN γ -mediated iNOS expression (a marker of M1-polarized macrophages) and increases iron-mediated toxicity [241], suggesting that a higher H-Fn expression in M1 macrophages contributes to the storage and detoxification of exogenously added iron.

As a product of the increase in \cdot NO production, the M1 phenotype also has quite different metabolic characteristics from the M2 phenotype. Nitric oxide induces disassembly of the [4Fe-4S] cluster on m-aconitase, breaking the flux along the tricarboxylic acid (TCA) cycle, thus triggering a reduction in pyruvate oxidation by pyruvate dehydrogenase and diminishing the protein levels and activity of mitochondrial electron transport chain complexes [242]. Therefore, the M1 phenotype supports energy metabolism based on the

oxidation of glucose by glycolysis and the subsequent conversion of pyruvate to lactate. Interestingly, treating microglia with FeCl₃ upregulates both the expression and activity of 6-phosphofructo-2-kinase/fructose-2,6-biphosphatase 3, which is an enzyme that controls fructose 2,6 biphosphate levels—the key stimulator of glycolytic flux—suggesting that increased glycolysis and iron retention are interrelated [69].

The iron-induced change to an M1 phenotype may represent an adaptive mechanism that allows microglia/macrophages to survive in a pro-oxidant environment, especially to survive their own ·NO production. The metabolic shift from oxidative phosphorylation to glycolysis decreases the production of ·O₂[−] by the mitochondria, which would otherwise react with ·NO to produce the highly toxic peroxynitrite molecule. Higher levels of H-Fn also protect M1 microglia/macrophages from iron-mediated oxidative stress. Supporting this hypothesis, the glycolytic signatures of LPS-treated macrophages are lost under low environmental oxygen tension [243]. Additionally, M2-polarized microglia are more sensitive to ferroptosis, which is an iron- and redox-driven cell death program [244]. M2 microglia have increased levels of 15-lipoxygenase (15-LOX)—an important enzyme for the synthesis of pro-resolving lipid mediators—which also catalyzes the production of an essential pro-ferroptosis lipid signal [245]. Suggestively, M1 resistance to ferroptosis depends on iNOS-mediated ·NO production, and ·NO treatment protects M2 microglia from ferroptosis [244]. The implications of the role of iron in the balance between M1/M2 phenotypes in neurodegenerative diseases remain largely unexplored.

In immortalized microglia, iron potentiates Aβ-induced IL1β secretion (an M1 cytokine) through an ROS- and NFκB-mediated pathway [246]. The Aβ peptide (like LPS and IFNγ) promotes M1 microglial polarization, concomitantly with an increase in NTBI uptake and elevated levels of DMT1 and H-Fn. Additionally, M1 microglia shift their metabolism toward glycolysis, increasing the production of lactate and extracellular acidity, and enhancing pH-dependent iron uptake through DMT1 [232,247]. These glycolytic and iron-retentive microglia are also observed in APP/PS1 transgenic mice [69,247]. Furthermore, in a PD mice model induced by paraquat and maneb, NE depletion by DSP-4 amplifies hippocampal microglial activation and M1 polarization and increases the iron content, correlated with the upregulation of TfR1 and downregulation of Fpn1 [26].

In mice deficient for the NFκB family member c-Rel, which show a late onset parkinsonism preceded by some prodromal PD symptoms, such as intestinal constipation and olfactory impairment [248], an increased expression of M2 microglia/macrophages markers is transiently observed in young, but not older, animals [249]. It remains to be established if this switch from an M2 phenotype to an inflammatory M1 phenotype is a consequence of iron overload caused by phagocytosis of iron-rich, neuromelanin-bearing neurons in the c-Rel KO mice, or of iron-loaded amyloid plaques in the APP/PS1 mice. Overall, the above results indicate that the modulation of M1/M2 polarization is a promising therapeutic alternative for reducing neuroinflammation and dopaminergic neuronal death [250]. Targeting the iron homeostasis regulatory mechanisms could be a feasible alternative.

6. A Synergistic Role of Iron Accumulation and Neuroinflammation in Neurodegeneration

Neuroinflammation and brain iron accumulation mutually enhance each other through multiple mechanisms. Beyond translational regulation mediated by the IRE/IRP system, iron transporters can be regulated at the transcriptional or post-translational level by inflammatory mediators. For example, ·NO can S-nitrosylate DMT1 at Cys23 and Cys540, increasing Fe²⁺-uptake activity [251]. Additionally, ·NO also regulates DMT1 protein levels through an indirect mechanism. Parkin, which is an E3 ubiquitin ligase involved in dopaminergic neuron survival, is S-nitrosylated in PD brains and MPTP-injected mice and this modification inhibits its function [252]. Parkin mediates the ubiquitylation of the DMT1B isoform [253,254]. Accordingly, S-nitrosylation of Parkin impairs DMT1 ubiquitylation, increasing DMT1 protein levels. Furthermore, treatment with MPP⁺ (the active metabolite of MPTP) results in Parkin S-nitrosylation and elevated DMT1 protein levels in Parkin-expressing human neuroblastoma cells. A similar effect is observed in the SN

of MPTP-injected mice [255]. Interestingly, neuronal DMT1 overexpression triggers an increase of Parkin levels in an apparent compensatory response [256].

The expression of DMT1 is transcriptionally enhanced by the transcription factor NF κ B [257], whose activation occurs downstream of many cytokine receptors, such as the TNF receptor (TNFR) and the IL1 receptor (IL1R). The activation of NF κ B by inflammatory stimuli may play a significant role in iron accumulation by dopaminergic neurons of the SN, which express high levels of TNFR [258]. Interestingly, an increase in the nuclear immunoreactivity of NF κ B was observed in PD patients' brains or in animal models of this disease [259]. Remarkably, treatment with ebselen, which is a selective DMT1 blocker, reduces iron deposition in the SN of LPS-treated mice and prevents neuronal loss and motor deficits [251], suggesting that DMT1-mediated iron entry is relevant in neuroinflammation-mediated neuronal death. Moreover, AD post-mortem tissue displays an increased expression and/or activation of NF κ B, particularly in regions preferentially affected in AD [260]. This increased expression correlates with an increased DMT1 expression, both in post-mortem tissue and in transgenic APPsw mice [261].

In PD, a self-perpetuating cycle between neurodegeneration and neuroinflammation is also sustained by neuromelanin (NM) released from dead dopaminergic neurons. Neuromelanin is an insoluble pigment formed by oxidized metabolites of dopamine with a remarkably avidity for Fe³⁺ ions that accumulates with aging, particularly in the SN and LC [262]. Neuromelanin-containing neurons are selectively vulnerable to neurodegeneration [263]. The engulfment of extracellular NM by microglia [264] induces NF κ B-dependent microglia activation [265], and triggers mesencephalic neuronal death [266].

The co-occurrence of iron accumulation and neuroinflammation can exacerbate neuronal death. Therefore, the use of iron chelators during neuroinflammation protects the brain from iron overload, reduces microglial activation, and improves cognitive functions in rodents [267–269]. As iron catalytically converts H₂O₂ and \cdot O₂⁻ to the highly toxic hydroxyl radical through the Haber–Weiss reaction, their accumulation could enhance neurotoxicity mediated by glial NOX products.

Iron also promotes microglial activation and NOX2-dependent \cdot O₂⁻ production, and in turn, microglia activation contributes to selective iron-mediated neurotoxicity in mixed midbrain-derived primary cultures [270]. NOX2 activation is also involved in paraquat-mediated microglial activation by iron, and microglial cells are essential for enhanced dopaminergic cell death triggered by paraquat/iron treatment [271]. In paraquat- and maneb-treated mice, the NOX inhibitor apocynin restores normal Fpn1 protein levels and inhibits iron accumulation, ameliorating neuroinflammation, lipid peroxidation, and dopaminergic neurodegeneration [272]. Similarly, iron also increases LPS-neurotoxicity when administered to co-cultures of primary neurons and microglia, and neuronal death can be reversed by NOX2 and NOX4 inhibition [273]. Preliminary results from our laboratory also show a synergistic role of neuroinflammation and iron in downstream oxidative stress (Figure 3).

Treatment of hippocampal neurons with pro-inflammatory cytokines (IL6 and TNF α) or with LPS increases the fraction of oxidized cysteines; this increase is abrogated by pre-treatment with the antioxidant N-acetylcysteine (NAC, Figure 3A,B). These changes make neurons more prone to oxidative damage, since an increase in their iron content, together with increased ROS production, fosters the production of the highly reactive hydroxyl radical. Accordingly, the detection of hydroxyl radicals with dichlorofluorescein (DCF) indicated that the pre-treatment with IL6, TNF α , or LPS enhanced its production after incubation with iron (Figure 3C). Hence, elevated levels of neuronal iron can act synergistically with cytokine-mediated ROS production to overwhelm antioxidant defenses.

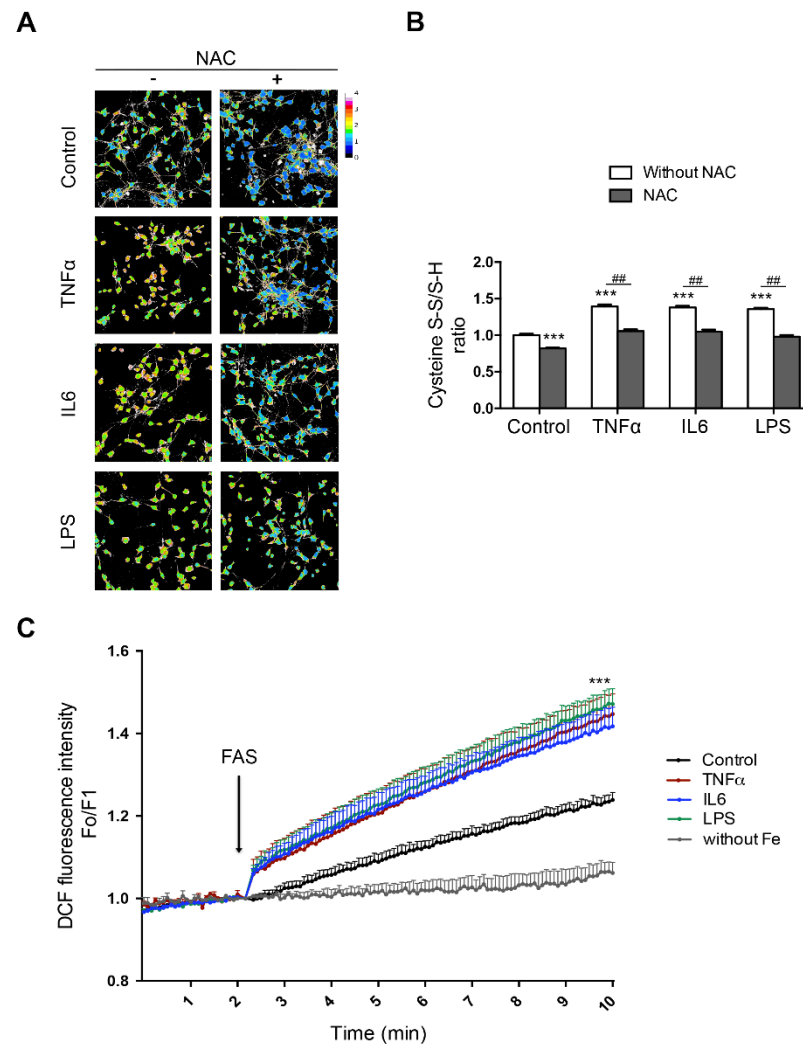


Figure 3. Pro-inflammatory cytokines enhance iron-mediated reactive oxygen species (ROS) production. Hippocampal neurons (7 DIV) were treated with tumor necrosis factor (TNF) α (50 ng/mL), IL6 (50 ng/mL), or lipopolysaccharide (LPS) (1 μ g/mL) for 18 h in the presence or absence of 0.5 mM N-acetylcysteine (NAC). (A) The oxidative tone was evaluated by the amount of reduced and oxidized cysteine in proteins. Maleimide-Alexa 488 (green) was used to detect reduced cysteines and maleimide-Alexa 568 (red) to detect oxidized cysteines. The ratio between red and green fluorescence was transformed (ImageJ program) into a thermal scale (right hand bar) in which a shift from blue to red to white implies a higher degree of oxidation. (B) Quantification of the reduced/oxidized cysteine ratio. (C) Increased dichlorofluorescein (DCF) fluorescence, which is a dye sensitive to ROS production, was evaluated after the addition of ferric ammonium sulfate (FAS). Fluorescence data were collected in a microfluorometer plate reader and the ratio between fluorescence (F) and initial fluorescence (F_o) was plotted. Values represent the mean \pm SEM ($n = 120$ neurons, from three independent experiments). *** $p < 0.001$ compared to the control and ## $p < 0.01$ compared with the conditions without or with NAC. For protocol detail see [137].

7. Conclusions

Connected through an intricate network of molecular interactions, neuroinflammation and iron accumulation establish a noxious circle that sustains the progressive neurodegeneration process observed in AD and PD (Figure 4). Iron promotes the M1 pro-inflammatory phenotype in microglia and macrophages, characterized by the expression of iNOS. Moreover, iNOS-mediated \cdot NO production is essential for the adaptive remodeling of iron homeostasis and metabolic pathways in M1 microglia/macrophages that concur to fer-

roptosis resistance. These changes make the endurance of neuroinflammation over time possible, even under oxidative stress conditions that would be toxic to neighboring cells such as neurons. Additionally, $\cdot\text{NO}$ can disrupt the Fe-S cluster in c-aconitase, activating IRP1, even in iron-sufficiency conditions, thus potentiating mitochondrial iron accumulation and oxidative stress, ultimately leading to neuronal death.

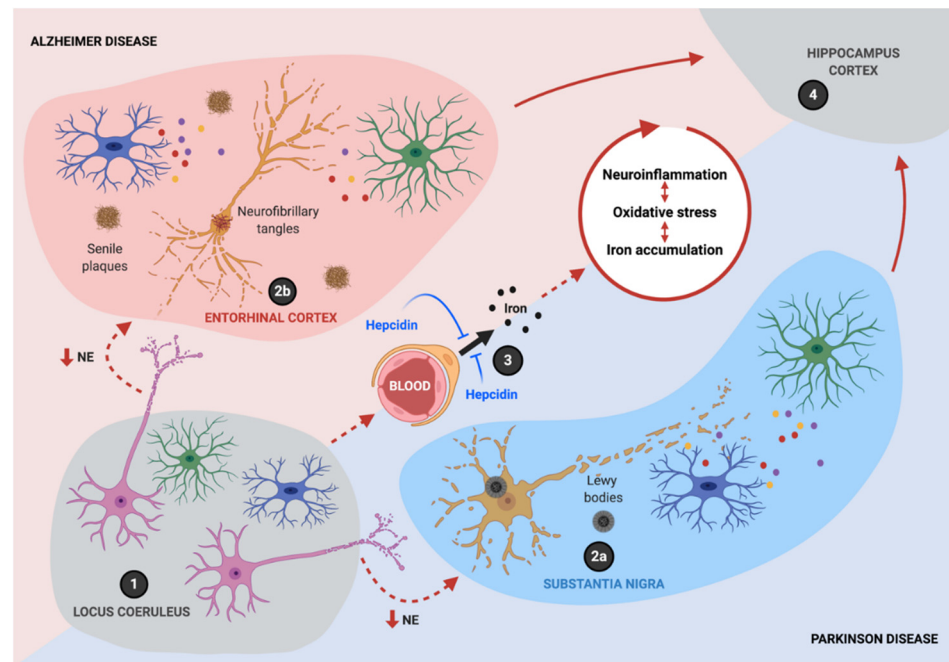


Figure 4. Iron and inflammation are intertwined in a bidirectional relationship during neurodegeneration. The neurodegenerative process starts with the loss of immune homeostatic mechanisms, partially due to decreased norepinephrine (NE) neurotransmission after the degeneration of the locus coeruleus (LC) (1). It continues with neuronal death in intrinsically sensitive areas, such as the substantia nigra (SN) (2a) and the entorhinal cortex (2b), fueled by a positive feedback loop between neuroinflammation, oxidative stress, and iron accumulation (the wheel at the center). As the disease progresses, neurodegeneration continues to other brain regions, such as the hippocampus and the cortex (4). Hepcidin can suppress the main pathologies in experimental Alzheimer's disease (AD) and Parkinson's disease (PD) through the inhibition of iron entry at the blood–brain barrier (BBB) (3). Created with BioRender.com.

Further knowledge on the molecular hierarchy that supports the relationship between neuroinflammation and iron overload will open new therapeutic avenues that allow for the disruption of this circle in AD and PD. Restraining iron entry to the CNS by hepcidin treatment and conservative brain iron chelation are two possible strategies for the treatment of these devastating diseases.

Author Contributions: P.J.U., D.A.B. and M.T.N. wrote the paper. All authors have read and agreed to the published version of the manuscript.

Funding: This research was funded by FONDECYT Initiation in Research, grant number 11201141, awarded to P.J.U.

Institutional Review Board Statement: The study was conducted according to the protocol for the handling of animals approved by the Ethics Committee for the Handling of Live Species and Biosafety of Faculty of Sciences of Universidad de Chile (Project approval n° 1100599, March 2010).

Informed Consent Statement: Not applicable.

Data Availability Statement: Not applicable.

Acknowledgments: We thank Cecilia Hidalgo for the critical reviewing of this paper.

Conflicts of Interest: The authors declare no conflict of interest.

References

1. Abe, N.; Nishihara, T.; Yorozuya, T.; Tanaka, J. Microglia and Macrophages in the Pathological Central and Peripheral Nervous Systems. *Cells* **2020**, *9*, 2132. [[CrossRef](#)] [[PubMed](#)]
2. Braak, H.; Ghebremedhin, E.; Rub, U.; Bratzke, H.; Del Tredici, K. Stages in the development of Parkinson's disease-related pathology. *Cell Tissue Res.* **2004**, *318*, 121–134. [[CrossRef](#)] [[PubMed](#)]
3. Sun, W.; Tang, Y.; Qiao, Y.; Ge, X.; Mather, M.; Ringman, J.M.; Shi, Y. A probabilistic atlas of locus coeruleus pathways to transentorhinal cortex for connectome imaging in Alzheimer's disease. *NeuroImage* **2020**, *223*, 117301. [[CrossRef](#)]
4. Braak, H.; Thal, D.R.; Ghebremedhin, E.; Del Tredici, K. Stages of the pathological process in Alzheimer disease: Age categories from 1 to 100 years. *J. Neuropathol. Exp. Neurol.* **2011**, *70*, 960–969. [[CrossRef](#)] [[PubMed](#)]
5. Theofilas, P.; Ehrenberg, A.J.; Dunlop, S.; Alho, A.T.D.L.; Nguy, A.; Leite, R.E.P.; Rodriguez, R.D.; Mejia, M.B.; Suemoto, C.K.; Ferretti-Rebustini, R.E.L.; et al. Locus coeruleus volume and cell population changes during Alzheimer's disease progression: A stereological study in human postmortem brains with potential implication for early-stage biomarker discovery. *Alzheimers Dement.* **2017**, *13*, 236–246. [[CrossRef](#)] [[PubMed](#)]
6. Kang, S.S.; Liu, X.; Ahn, E.H.; Xiang, J.; Manfredsson, F.P.; Yang, X.; Luo, H.R.; Liles, L.C.; Weinshenker, D.; Ye, K. Norepinephrine metabolite DOPEGAL activates AEP and pathological Tau aggregation in locus coeruleus. *J. Clin. Investig.* **2020**, *130*, 422–437. [[CrossRef](#)] [[PubMed](#)]
7. Wang, Q.; Oyarzabal, E.A.; Song, S.; Wilson, B.; Santos, J.H.; Hong, J.S. Locus coeruleus neurons are most sensitive to chronic neuroinflammation-induced neurodegeneration. *Brain Behav. Immun.* **2020**, *87*, 359–368. [[CrossRef](#)]
8. Song, S.; Jiang, L.; Oyarzabal, E.A.; Wilson, B.; Li, Z.; Shih, Y.I.; Wang, Q.; Hong, J.S. Loss of Brain Norepinephrine Elicits Neuroinflammation-Mediated Oxidative Injury and Selective Caudo-Rostral Neurodegeneration. *Mol. Neurobiol.* **2019**, *56*, 2653–2669. [[CrossRef](#)]
9. Horsager, J.; Andersen, K.B.; Knudsen, K.; Skjaerbaek, C.; Fedorova, T.D.; Okkels, N.; Schaeffer, E.; Bonkat, S.K.; Geday, J.; Otto, M.; et al. Brain-first versus body-first Parkinson's disease: A multimodal imaging case-control study. *Brain* **2020**, *143*, 3077–3088. [[CrossRef](#)]
10. Jiang, L.; Chen, S.-H.; Chu, C.-H.; Wang, S.-J.; Oyarzabal, E.; Wilson, B.; Sanders, V.; Xie, K.; Wang, Q.; Hong, J.-S. A novel role of microglial NADPH oxidase in mediating extra-synaptic function of norepinephrine in regulating brain immune homeostasis. *Glia* **2015**, *63*, 1057–1072. [[CrossRef](#)]
11. Yssel, J.D.; O'Neill, E.; Nolan, Y.M.; Connor, T.J.; Harkin, A. Treatment with the noradrenaline re-uptake inhibitor atomoxetine alone and in combination with the alpha2-adrenoceptor antagonist idazoxan attenuates loss of dopamine and associated motor deficits in the LPS inflammatory rat model of Parkinson's disease. *Brain Behav. Immun.* **2018**, *69*, 456–469. [[CrossRef](#)]
12. Bharani, K.L.; Derex, R.; Granholm, A.C.; Ledreux, A. A noradrenergic lesion aggravates the effects of systemic inflammation on the hippocampus of aged rats. *PLoS ONE* **2017**, *12*, e0189821. [[CrossRef](#)]
13. Liu, Y.U.; Ying, Y.; Li, Y.; Eyo, U.B.; Chen, T.; Zheng, J.; Umpierre, A.D.; Zhu, J.; Bosco, D.B.; Dong, H.; et al. Neuronal network activity controls microglial process surveillance in awake mice via norepinephrine signaling. *Nat. Neurosci.* **2019**, *22*, 1771–1781. [[CrossRef](#)] [[PubMed](#)]
14. Stowell, R.D.; Sipe, G.O.; Dawes, R.P.; Batchelor, H.N.; Lordy, K.A.; Whitelaw, B.S.; Stoessel, M.B.; Bidlack, J.M.; Brown, E.; Sur, M.; et al. Noradrenergic signaling in the wakeful state inhibits microglial surveillance and synaptic plasticity in the mouse visual cortex. *Nat. Neurosci.* **2019**, *22*, 1782–1792. [[CrossRef](#)]
15. Heneka, M.T.; Galea, E.; Gavriluyk, V.; Dumitrescu-Ozimek, L.; Daeschner, J.; O'Banion, M.K.; Weinberg, G.; Klockgether, T.; Feinstein, D.L. Noradrenergic depletion potentiates beta-amyloid-induced cortical inflammation: Implications for Alzheimer's disease. *J. Neurosci.* **2002**, *22*, 2434–2442. [[CrossRef](#)] [[PubMed](#)]
16. Song, S.; Wang, Q.; Jiang, L.; Oyarzabal, E.; Riddick, N.V.; Wilson, B.; Moy, S.S.; Shih, Y.I.; Hong, J.S. Noradrenergic dysfunction accelerates LPS-elicited inflammation-related ascending sequential neurodegeneration and deficits in non-motor/motor functions. *Brain Behav. Immun.* **2019**, *81*, 374–387. [[CrossRef](#)]
17. Yao, N.; Wu, Y.; Zhou, Y.; Ju, L.; Liu, Y.; Ju, R.; Duan, D.; Xu, Q. Lesion of the locus coeruleus aggravates dopaminergic neuron degeneration by modulating microglial function in mouse models of Parkinsons disease. *Brain Res.* **2015**, *1625*, 255–274. [[CrossRef](#)] [[PubMed](#)]
18. Song, S.; Liu, J.; Zhang, F.; Hong, J.S. Norepinephrine depleting toxin DSP-4 and LPS alter gut microbiota and induce neurotoxicity in alpha-synuclein mutant mice. *Sci. Rep.* **2020**, *10*, 1–13. [[CrossRef](#)]
19. Heneka, M.T.; Ramanathan, M.; Jacobs, A.H.; Dumitrescu-Ozimek, L.; Bilkei-Gorzo, A.; Debeir, T.; Sastre, M.; Galldiks, N.; Zimmer, A.; Hoehn, M.; et al. Locus ceruleus degeneration promotes Alzheimer pathogenesis in amyloid precursor protein 23 transgenic mice. *J. Neurosci.* **2006**, *26*, 1343–1354. [[CrossRef](#)]
20. Kalinin, S.; Gavriluyk, V.; Polak, P.E.; Vasser, R.; Zhao, J.; Heneka, M.T.; Feinstein, D.L. Noradrenaline deficiency in brain increases beta-amyloid plaque burden in an animal model of Alzheimer's disease. *Neurobiol. Aging* **2007**, *28*, 1206–1214. [[CrossRef](#)]

21. Heneka, M.T.; Nadrigny, F.; Regen, T.; Martinez-Hernandez, A.; Dumitrescu-Ozimek, L.; Terwel, D.; Jardanhazi-Kurutz, D.; Walter, J.; Kirchhoff, F.; Hanisch, U.K.; et al. Locus ceruleus controls Alzheimer's disease pathology by modulating microglial functions through norepinephrine. *Proc. Natl. Acad. Sci. USA* **2010**, *107*, 6058–6063. [[CrossRef](#)] [[PubMed](#)]
22. Duffy, K.B.; Ray, B.; Lahiri, D.K.; Tilmont, E.M.; Tinkler, G.P.; Herbert, R.L.; Greig, N.H.; Ingram, D.K.; Ottinger, M.A.; Mattison, J.A. Effects of Reducing Norepinephrine Levels via DSP4 Treatment on Amyloid-beta Pathology in Female Rhesus Macaques (Macaca Mulatta). *J. Alzheimers Dis.* **2019**, *68*, 115–126. [[CrossRef](#)] [[PubMed](#)]
23. Ghosh, A.; Torraville, S.E.; Mukherjee, B.; Walling, S.G.; Martin, G.M.; Harley, C.W.; Yuan, Q. An experimental model of Braak's pretangle proposal for the origin of Alzheimer's disease: The role of locus coeruleus in early symptom development. *Alzheimers Res. Ther.* **2019**, *11*, 1–17. [[CrossRef](#)] [[PubMed](#)]
24. Bjerken, S.A.; Persson, R.S.; Barkander, A.; Karalija, N.; Pelegrina-Hidalgo, N.; Gerhardt, G.A.; Virel, A.; Stromberg, I. Norepinephrine is crucial for the substantia nigra dopaminergic cell maintenance. *Neurochem. Int.* **2019**, *131*, 104551. [[CrossRef](#)]
25. Evans, A.K.; Ardestani, P.M.; Yi, B.; Park, H.H.; Lam, R.K.; Shamloo, M. Beta-adrenergic receptor antagonism is proinflammatory and exacerbates neuroinflammation in a mouse model of Alzheimer's Disease. *Neurobiol. Dis.* **2020**, *146*, 105089. [[CrossRef](#)]
26. Hou, L.; Sun, F.; Sun, W.; Zhang, L.; Wang, Q. Lesion of the Locus Coeruleus Damages Learning and Memory Performance in Paraquat and Maneb-induced Mouse Parkinson's Disease Model. *Neuroscience* **2019**, *419*, 129–140. [[CrossRef](#)]
27. Zammit, M.; Tao, Y.; Olsen, M.E.; Metzger, J.; Vermilyea, S.C.; Bjornson, K.; Slesarev, M.; Block, W.F.; Fuchs, K.; Phillips, S.; et al. [(18)F]FEPPA PET imaging for monitoring CD68-positive microglia/macrophage neuroinflammation in nonhuman primates. *EJNMMI Res.* **2020**, *10*, 93. [[CrossRef](#)]
28. Joers, V.; Masilamoni, G.; Kempf, D.; Weiss, A.R.; Rotterman, T.M.; Murray, B.; Yalcin-Cakmakli, G.; Voll, R.J.; Goodman, M.M.; Howell, L.; et al. Microglia, inflammation and gut microbiota responses in a progressive monkey model of Parkinson's disease: A case series. *Neurobiol. Dis.* **2020**, *144*, 105027. [[CrossRef](#)]
29. Rodriguez-Chinchilla, T.; Quiroga-Varela, A.; Molinet-Dronca, F.; Belloso-Iguerategui, A.; Merino-Galan, L.; Jimenez-Urbieta, H.; Gago, B.; Rodriguez-Oroz, M.C. [(18)F]-DPA-714 PET as a specific in vivo marker of early microglial activation in a rat model of progressive dopaminergic degeneration. *Eur. J. Nucl. Med. Mol. Imaging* **2020**, *47*, 2602–2612. [[CrossRef](#)]
30. Crabbe, M.; Van Der Perren, A.; Bollaerts, I.; Kounelis, S.; Baekelandt, V.; Bormans, G.; Casteels, C.; Moons, L.; Van Laere, K. Increased P2X7 Receptor Binding Is Associated With Neuroinflammation in Acute but Not Chronic Rodent Models for Parkinson's Disease. *Front. Neurosci.* **2019**, *13*, 799. [[CrossRef](#)]
31. Wu, C.Y.; Chen, Y.Y.; Lin, J.J.; Li, J.P.; Chen, J.K.; Hsieh, T.C.; Kao, C.H. Development of a novel radioligand for imaging 18-kD translocator protein (TSPO) in a rat model of Parkinson's disease. *BMC Med. Imaging* **2019**, *19*, 78. [[CrossRef](#)]
32. Vetel, S.; Serriere, S.; Vercouillie, J.; Vergote, J.; Chicheri, G.; Deloye, J.B.; Dolle, F.; Bodard, S.; Tronel, C.; Nadal-Desbarats, L.; et al. Extensive exploration of a novel rat model of Parkinson's disease using partial 6-hydroxydopamine lesion of dopaminergic neurons suggests new therapeutic approaches. *Synapse* **2019**, *73*, e22077. [[CrossRef](#)] [[PubMed](#)]
33. Sun, L.; Shen, R.; Agnihotri, S.K.; Chen, Y.; Huang, Z.; Bueler, H. Lack of PINK1 alters glia innate immune responses and enhances inflammation-induced, nitric oxide-mediated neuron death. *Sci. Rep.* **2018**, *8*, 383. [[CrossRef](#)] [[PubMed](#)]
34. Chien, C.H.; Lee, M.J.; Liou, H.C.; Liou, H.H.; Fu, W.M. Microglia-Derived Cytokines/Chemokines Are Involved in the Enhancement of LPS-Induced Loss of Nigrostriatal Dopaminergic Neurons in DJ-1 Knockout Mice. *PLoS ONE* **2016**, *11*, e0151569. [[CrossRef](#)] [[PubMed](#)]
35. Hu, W.; Pan, D.; Wang, Y.; Bao, W.; Zuo, C.; Guan, Y.; Hua, F.; Yang, M.; Zhao, J. PET Imaging for Dynamically Monitoring Neuroinflammation in APP/PS1 Mouse Model Using [(18)F]DPA714. *Front. Neurosci.* **2020**, *14*, 810. [[CrossRef](#)] [[PubMed](#)]
36. Sacher, C.; Blume, T.; Beyers, L.; Peters, F.; Eckenweber, F.; Sgobio, C.; Deussing, M.; Albert, N.L.; Unterrainer, M.; Lindner, S.; et al. Longitudinal PET Monitoring of Amyloidosis and Microglial Activation in a Second-Generation Amyloid-beta Mouse Model. *J. Nucl. Med.* **2019**, *60*, 1787–1793. [[CrossRef](#)]
37. Tournier, B.B.; Tsartsalis, S.; Ceyzeriat, K.; Garibotto, V.; Millet, P. In Vivo TSPO Signal and Neuroinflammation in Alzheimer's Disease. *Cells* **2020**, *9*, 1941. [[CrossRef](#)]
38. Belloli, S.; Morari, M.; Murtaj, V.; Valtorta, S.; Moresco, R.M.; Gilardi, M.C. Translation Imaging in Parkinson's Disease: Focus on Neuroinflammation. *Front. Aging Neurosci.* **2020**, *12*, 152. [[CrossRef](#)] [[PubMed](#)]
39. Pannell, M.; Economopoulos, V.; Wilson, T.C.; Kersemans, V.; Isenegger, P.G.; Larkin, J.R.; Smart, S.; Gilchrist, S.; Gouverneur, V.; Sibson, N.R. Imaging of translocator protein upregulation is selective for pro-inflammatory polarized astrocytes and microglia. *Glia* **2020**, *68*, 280–297. [[CrossRef](#)]
40. Tournier, B.B.; Tsartsalis, S.; Ceyzeriat, K.; Medina, Z.; Fraser, B.H.; Gregoire, M.C.; Kovari, E.; Millet, P. Fluorescence-activated cell sorting to reveal the cell origin of radioligand binding. *J. Cereb. Blood Flow Metab.* **2020**, *40*, 1242–1255. [[CrossRef](#)]
41. Owen, D.R.; Yeo, A.J.; Gunn, R.N.; Song, K.; Wadsworth, G.; Lewis, A.; Rhodes, C.; Pulford, D.J.; Bennacef, I.; Parker, C.A.; et al. An 18-kDa translocator protein (TSPO) polymorphism explains differences in binding affinity of the PET radioligand PBR28. *J. Cereb. Blood Flow Metab.* **2012**, *32*, 1–5. [[CrossRef](#)] [[PubMed](#)]
42. Laurell, G.L.; Plaven-Sigray, P.; Jucaite, A.; Varrone, A.; Cosgrove, K.P.; Svarer, C.; Knudsen, G.M.; Ogden, R.T.; Zanderigo, F.; Cervenka, S.; et al. Non-displaceable binding is a potential confounding factor in (11)CPBR28 TSPO PET studies. *J. Nucl. Med.* **2020**, *10*. [[CrossRef](#)]

43. Kim, S.W.; Wiers, C.E.; Tyler, R.; Shokri-Kojori, E.; Jang, Y.J.; Zehra, A.; Freeman, C.; Ramirez, V.; Lindgren, E.; Miller, G.; et al. Influence of alcoholism and cholesterol on TSPO binding in brain: PET [(11)C]PBR28 studies in humans and rodents. *Neuropsychopharmacology* **2018**, *43*, 1832–1839. [[CrossRef](#)] [[PubMed](#)]
44. Tournier, B.B.; Tsartsalis, S.; Ceyzeriat, K.; Fraser, B.H.; Gregoire, M.C.; Kovari, E.; Millet, P. Astrocytic TSPO Upregulation Appears Before Microglial TSPO in Alzheimer's Disease. *J. Alzheimers Dis.* **2020**, *77*, 1043–1056. [[CrossRef](#)]
45. Gong, P.; Chen, Y.Q.; Lin, A.H.; Zhang, H.B.; Zhang, Y.; Ye, R.D.; Yu, Y. p47(phox) deficiency improves cognitive impairment and attenuates tau hyperphosphorylation in mouse models of AD. *Alzheimers Res. Ther.* **2020**, *12*, 146. [[CrossRef](#)]
46. Geng, L.; Fan, L.M.; Liu, F.; Smith, C.; Li, J. Nox2 dependent redox-regulation of microglial response to amyloid-beta stimulation and microgliosis in aging. *Sci. Rep.* **2020**, *10*, 1582. [[CrossRef](#)]
47. Liberatore, G.T.; Jackson-Lewis, V.; Vukosavic, S.; Mandir, A.S.; Vila, M.; McAuliffe, W.G.; Dawson, V.L.; Dawson, T.M.; Przedborski, S. Inducible nitric oxide synthase stimulates dopaminergic neurodegeneration in the MPTP model of Parkinson disease. *Nat. Med.* **1999**, *5*, 1403–1409. [[CrossRef](#)]
48. Dehmer, T.; Lindenau, J.; Haid, S.; Dichgans, J.; Schulz, J.B. Deficiency of inducible nitric oxide synthase protects against MPTP toxicity in vivo. *J. Neurochem.* **2000**, *74*, 2213–2216. [[CrossRef](#)]
49. Smith, T.S.; Swerdlow, R.H.; Parker, W.D., Jr.; Bennett, J.P., Jr. Reduction of MPP(+)-induced hydroxyl radical formation and nigrostriatal MPTP toxicity by inhibiting nitric oxide synthase. *Neuroreport* **1994**, *5*, 2598–2600. [[CrossRef](#)]
50. Qin, L.; Liu, Y.; Wang, T.; Wei, S.J.; Block, M.L.; Wilson, B.; Liu, B.; Hong, J.S. NADPH oxidase mediates lipopolysaccharide-induced neurotoxicity and proinflammatory gene expression in activated microglia. *J. Biol. Chem.* **2004**, *279*, 1415–1421. [[CrossRef](#)]
51. McGeer, P.L.; Schulzer, M.; McGeer, E.G. Arthritis and anti-inflammatory agents as possible protective factors for Alzheimer's disease: A review of 17 epidemiologic studies. *Neurology* **1996**, *47*, 425–432. [[CrossRef](#)]
52. Wang, J.; Tan, L.; Wang, H.F.; Tan, C.C.; Meng, X.F.; Wang, C.; Tang, S.W.; Yu, J.T. Anti-inflammatory drugs and risk of Alzheimer's disease: An updated systematic review and meta-analysis. *J. Alzheimers Dis.* **2015**, *44*, 385–396. [[CrossRef](#)] [[PubMed](#)]
53. Gagne, J.J.; Power, M.C. Anti-inflammatory drugs and risk of Parkinson disease: A meta-analysis. *Neurology* **2010**, *74*, 995–1002. [[CrossRef](#)] [[PubMed](#)]
54. Moore, A.H.; Bigbee, M.J.; Boynton, G.E.; Wakeham, C.M.; Rosenheim, H.M.; Staral, C.J.; Morrissey, J.L.; Hund, A.K. Non-Steroidal Anti-Inflammatory Drugs in Alzheimer's Disease and Parkinson's Disease: Reconsidering the Role of Neuroinflammation. *Pharmaceuticals* **2010**, *3*, 1812–1841. [[CrossRef](#)] [[PubMed](#)]
55. Sofic, E.; Riederer, P.; Heinsen, H.; Beckmann, H.; Reynolds, G.P.; Hebenstreit, G.; Youdim, M.B. Increased iron (III) and total iron content in post mortem substantia nigra of parkinsonian brain. *J. Neural Transm.* **1988**, *74*, 199–205. [[CrossRef](#)] [[PubMed](#)]
56. Griffiths, P.D.; Crossman, A.R. Distribution of iron in the basal ganglia and neocortex in postmortem tissue in Parkinson's disease and Alzheimer's disease. *Dementia* **1993**, *4*, 61–65. [[CrossRef](#)]
57. Connor, J.R.; Menzies, S.L.; St Martin, S.M.; Mufson, E.J. A histochemical study of iron, transferrin, and ferritin in Alzheimer's diseased brains. *J. Neurosci. Res.* **1992**, *31*, 75–83. [[CrossRef](#)]
58. Grundke-Iqbal, I.; Fleming, J.; Tung, Y.C.; Lassmann, H.; Iqbal, K.; Joshi, J.G. Ferritin is a component of the neuritic (senile) plaque in Alzheimer dementia. *Acta Neuropathol.* **1990**, *81*, 105–110. [[CrossRef](#)]
59. Dexter, D.T.; Carayon, A.; Javoy-Agid, F.; Agid, Y.; Wells, F.R.; Daniel, S.E.; Lees, A.J.; Jenner, P.; Marsden, C.D. Alterations in the levels of iron, ferritin and other trace metals in Parkinson's disease and other neurodegenerative diseases affecting the basal ganglia. *Brain* **1991**, *114*, 1953–1975. [[CrossRef](#)]
60. Kasarskis, E.J.; Tandon, L.; Lovell, M.A.; Ehmann, W.D. Aluminum, calcium, and iron in the spinal cord of patients with sporadic amyotrophic lateral sclerosis using laser microprobe mass spectroscopy: A preliminary study. *J. Neurol. Sci.* **1995**, *130*, 203–208. [[CrossRef](#)]
61. Arribarat, G.; De Barros, A.; Peran, P. Modern Brainstem MRI Techniques for the Diagnosis of Parkinson's Disease and Parkinsonisms. *Front. Neurol.* **2020**, *11*, 791. [[CrossRef](#)] [[PubMed](#)]
62. Barbosa, J.H.; Santos, A.C.; Tumas, V.; Liu, M.; Zheng, W.; Haacke, E.M.; Salmon, C.E. Quantifying brain iron deposition in patients with Parkinson's disease using quantitative susceptibility mapping, R2 and R2. *Magn. Reson. Imaging* **2015**, *33*, 559–565. [[CrossRef](#)] [[PubMed](#)]
63. Pyatigorskaya, N.; Sanz-Morere, C.B.; Gaurav, R.; Biondetti, E.; Valabregue, R.; Santin, M.; Yahia-Cherif, L.; Lehericy, S. Iron Imaging as a Diagnostic Tool for Parkinson's Disease: A Systematic Review and Meta-Analysis. *Front. Neurol.* **2020**, *11*, 366. [[CrossRef](#)] [[PubMed](#)]
64. Wang, X.; Zhang, Y.; Zhu, C.; Li, G.; Kang, J.; Chen, F.; Yang, L. The diagnostic value of SNpc using NM-MRI in Parkinson's disease: Meta-analysis. *Neurol. Sci.* **2019**, *40*, 2479–2489. [[CrossRef](#)] [[PubMed](#)]
65. Wang, J.Y.; Zhuang, Q.Q.; Zhu, L.B.; Zhu, H.; Li, T.; Li, R.; Chen, S.F.; Huang, C.P.; Zhang, X.; Zhu, J.H. Meta-analysis of brain iron levels of Parkinson's disease patients determined by postmortem and MRI measurements. *Sci. Rep.* **2016**, *6*, 36669. [[CrossRef](#)]
66. Du, L.; Zhao, Z.; Cui, A.; Zhu, Y.; Zhang, L.; Liu, J.; Shi, S.; Fu, C.; Han, X.; Gao, W.; et al. Increased Iron Deposition on Brain Quantitative Susceptibility Mapping Correlates with Decreased Cognitive Function in Alzheimer's Disease. *ACS Chem. Neurosci.* **2018**, *9*, 1849–1857. [[CrossRef](#)] [[PubMed](#)]
67. Pyatigorskaya, N.; Sharman, M.; Corvol, J.C.; Valabregue, R.; Yahia-Cherif, L.; Poupon, F.; Cormier-Dequaire, F.; Siebner, H.; Klebe, S.; Vidailhet, M.; et al. High nigral iron deposition in LRRK2 and Parkin mutation carriers using R2* relaxometry. *Mov. Disord.* **2015**, *30*, 1077–1084. [[CrossRef](#)]

68. Svobodova, H.; Kosnac, D.; Balazsiova, Z.; Tanila, H.; Miettinen, P.O.; Sierra, A.; Vitovic, P.; Wagner, A.; Polak, S.; Kopani, M. Elevated age-related cortical iron, ferritin and amyloid plaques in APP(swe)/PS1(deltaE9) transgenic mouse model of Alzheimer's disease. *Physiol. Res.* **2019**, *68*, S445–S451. [[CrossRef](#)]
69. McIntosh, A.; Mela, V.; Harty, C.; Minogue, A.M.; Costello, D.A.; Kerskens, C.; Lynch, M.A. Iron accumulation in microglia triggers a cascade of events that leads to altered metabolism and compromised function in APP/PS1 mice. *Brain Pathol.* **2019**, *29*, 606–621. [[CrossRef](#)]
70. Telling, N.D.; Everett, J.; Collingwood, J.F.; Dobson, J.; van der Laan, G.; Gallagher, J.J.; Wang, J.; Hitchcock, A.P. Iron Biochemistry is Correlated with Amyloid Plaque Morphology in an Established Mouse Model of Alzheimer's Disease. *Cell Chem. Biol.* **2017**, *24*, 1205–1215.e1203. [[CrossRef](#)]
71. Dong, X.-H.; Gao, W.-J.; Shao, T.-M.; Xie, H.-l.; Bai, J.-T.; Zhao, J.Y.; Chai, X.-Q. Age-related changes of brain iron load changes in the frontal cortex in APPswe/PS1DeltaE9 transgenic mouse model of Alzheimer's disease. *J. Trace Elem. Med. Biol.* **2015**, *30*, 118–123. [[CrossRef](#)]
72. Gurel, B.; Cansev, M.; Sevinc, C.; Kelestemur, S.; Ocalan, B.; Cakir, A.; Aydin, S.; Kahveci, N.; Ozansoy, M.; Taskapilioglu, O.; et al. Early Stage Alterations in CA1 Extracellular Region Proteins Indicate Dysregulation of IL6 and Iron Homeostasis in the 5XFAD Alzheimer's Disease Mouse Model. *J. Alzheimers Dis.* **2018**, *61*, 1399–1410. [[CrossRef](#)] [[PubMed](#)]
73. Mochizuki, H.; Imai, H.; Endo, K.; Yokomizo, K.; Murata, Y.; Hattori, N.; Mizuno, Y. Iron accumulation in the substantia nigra of 1-methyl-4-phenyl-1,2,3,6-tetrahydropyridine (MPTP)-induced hemiparkinsonian monkeys. *Neurosci. Lett.* **1994**, *168*, 251–253. [[CrossRef](#)] [[PubMed](#)]
74. Xiong, P.; Chen, X.; Guo, C.; Zhang, N.; Ma, B. Baicalin and deferoxamine alleviate iron accumulation in different brain regions of Parkinson's disease rats. *Neural Regen. Res.* **2012**, *7*, 2092–2098. [[CrossRef](#)]
75. Oestreicher, E.; Sengstock, G.J.; Riederer, P.; Olanow, C.W.; Dunn, A.J.; Arendash, G.W. Degeneration of nigrostriatal dopaminergic neurons increases iron within the substantia nigra: A histochemical and neurochemical study. *Brain Res.* **1994**, *660*, 8–18. [[CrossRef](#)]
76. Kaur, D.; Peng, J.; Chinta, S.J.; Rajagopalan, S.; Di Monte, D.A.; Cherny, R.A.; Andersen, J.K. Increased murine neonatal iron intake results in Parkinson-like neurodegeneration with age. *Neurobiol. Aging* **2007**, *28*, 907–913. [[CrossRef](#)]
77. Huang, C.; Ma, W.; Luo, Q.; Shi, L.; Xia, Y.; Lao, C.; Liu, W.; Zou, Y.; Cheng, A.; Shi, R.; et al. Iron overload resulting from the chronic oral administration of ferric citrate induces parkinsonism phenotypes in middle-aged mice. *Aging* **2019**, *11*, 9846–9861. [[CrossRef](#)]
78. Ben-Shachar, D.; Eshel, G.; Finberg, J.P.; Youdim, M.B. The iron chelator desferrioxamine (Desferal) retards 6-hydroxydopamine-induced degeneration of nigrostriatal dopamine neurons. *J. Neurochem.* **1991**, *56*, 1441–1444. [[CrossRef](#)]
79. Kaur, D.; Yantiri, F.; Rajagopalan, S.; Kumar, J.; Mo, J.Q.; Boonplueang, R.; Viswanath, V.; Jacobs, R.; Yang, L.; Beal, M.F.; et al. Genetic or pharmacological iron chelation prevents MPTP-induced neurotoxicity in vivo: A novel therapy for Parkinson's disease. *Neuron* **2003**, *37*, 899–909. [[CrossRef](#)]
80. Youdim, M.B.; Stephenson, G.; Ben Shachar, D. Ironing iron out in Parkinson's disease and other neurodegenerative diseases with iron chelators: A lesson from 6-hydroxydopamine and iron chelators, desferal and VK-28. *Ann. N. Y. Acad. Sci.* **2004**, *1012*, 306–325. [[CrossRef](#)]
81. Mena, N.P.; Garcia-Beltran, O.; Lourido, F.; Urrutia, P.J.; Mena, R.; Castro-Castillo, V.; Cassels, B.K.; Nunez, M.T. The novel mitochondrial iron chelator 5-((methylamino)methyl)-8-hydroxyquinoline protects against mitochondrial-induced oxidative damage and neuronal death. *Biochem. Biophys. Res. Commun.* **2015**, *463*, 787–792. [[CrossRef](#)] [[PubMed](#)]
82. Rao, S.S.; Portbury, S.D.; Lago, L.; Bush, A.I.; Adlard, P.A. The Iron Chelator Deferiprone Improves the Phenotype in a Mouse Model of Tauopathy. *J. Alzheimers. Dis.* **2020**, *77*, 753–771. [[CrossRef](#)]
83. Devos, D.; Moreau, C.; Devedjian, J.C.; Kluza, J.; Petraut, M.; Laloux, C.; Jonneaux, A.; Ryckewaert, G.; Garcon, G.; Rouaix, N.; et al. Targeting chelatable iron as a therapeutic modality in Parkinson's disease. *Antioxid. Redox. Signal.* **2014**, *21*, 195–210. [[CrossRef](#)]
84. Martin-Bastida, A.; Ward, R.J.; Newbould, R.; Piccini, P.; Sharp, D.; Kabba, C.; Patel, M.C.; Spino, M.; Connelly, J.; Tricta, F.; et al. Brain iron chelation by deferiprone in a phase 2 randomised double-blinded placebo controlled clinical trial in Parkinson's disease. *Sci. Rep.* **2017**, *7*, 1398. [[CrossRef](#)]
85. Nunez, M.T.; Chana-Cuevas, P. New Perspectives in Iron Chelation Therapy for the Treatment of Neurodegenerative Diseases. *Pharmaceuticals* **2018**, *11*, 109. [[CrossRef](#)]
86. Nunez, M.T.; Chana-Cuevas, P. New perspectives in iron chelation therapy for the treatment of Parkinson's disease. *Neural Regen. Res.* **2019**, *14*, 1905–1906. [[CrossRef](#)] [[PubMed](#)]
87. Ashraf, A.; Michaelides, C.; Walker, T.A.; Ekonomou, A.; Suessmilch, M.; Sriskanthanathan, A.; Abraha, S.; Parkes, A.; Parkes, H.G.; Geraki, K.; et al. Regional Distributions of Iron, Copper and Zinc and Their Relationships With Glia in a Normal Aging Mouse Model. *Front. Aging Neurosci.* **2019**, *11*, 351. [[CrossRef](#)]
88. Rodriguez-Callejas, J.D.; Cuervo-Zanatta, D.; Rosas-Arellano, A.; Fonta, C.; Fuchs, E.; Perez-Cruz, C. Loss of ferritin-positive microglia relates to increased iron, RNA oxidation, and dystrophic microglia in the brains of aged male marmosets. *Am. J. Primatol.* **2019**, *81*, e22956. [[CrossRef](#)] [[PubMed](#)]
89. Daugherty, A.M.; Hoagey, D.A.; Kennedy, K.M.; Rodrigue, K.M. Genetic predisposition for inflammation exacerbates effects of striatal iron content on cognitive switching ability in healthy aging. *NeuroImage* **2019**, *185*, 471–478. [[CrossRef](#)]

90. Ashraf, A.; Clark, M.; So, P.W. The Aging of Iron Man. *Front. Aging Neurosci.* **2018**, *10*, 65. [[CrossRef](#)] [[PubMed](#)]
91. Andreini, C.; Putignano, V.; Rosato, A.; Banci, L. The human iron-proteome. *Metallomics* **2018**, *10*, 1223–1231. [[CrossRef](#)] [[PubMed](#)]
92. Halliwell, B. Biochemistry of oxidative stress. *Biochem. Soc. Trans.* **2007**, *35*, 1147–1150. [[CrossRef](#)] [[PubMed](#)]
93. Johnsen, K.B.; Burkhart, A.; Thomsen, L.B.; Andresen, T.L.; Moos, T. Targeting the transferrin receptor for brain drug delivery. *Prog. Neurobiol.* **2019**, *181*, 101665. [[CrossRef](#)] [[PubMed](#)]
94. Duck, K.A.; Connor, J.R. Iron uptake and transport across physiological barriers. *Biometals* **2016**, *29*, 573–591. [[CrossRef](#)] [[PubMed](#)]
95. Arosio, P.; Ingrassia, R.; Cavadini, P. Ferritins: A family of molecules for iron storage, antioxidation and more. *Biochim. Biophys. Acta* **2009**, *1790*, 589–599. [[CrossRef](#)] [[PubMed](#)]
96. McCarthy, R.C.; Kosman, D.J. Iron transport across the blood-brain barrier: Development, neurovascular regulation and cerebral amyloid angiopathy. *Cell Mol. Life Sci.* **2015**, *72*, 709–727. [[CrossRef](#)]
97. Qian, Z.M.; Ke, Y. Brain iron transport. *Biol. Rev. Camb. Philos. Soc.* **2019**, *94*, 1672–1684. [[CrossRef](#)]
98. Wade, Q.W.; Chiou, B.; Connor, J.R. Iron uptake at the blood-brain barrier is influenced by sex and genotype. *Adv. Pharmacol.* **2019**, *84*, 123–145. [[CrossRef](#)]
99. Skarlatos, S.; Yoshikawa, T.; Pardridge, W.M. Transport of [125I]transferrin through the rat blood-brain barrier. *Brain Res.* **1995**, *683*, 164–171. [[CrossRef](#)]
100. Cohen, L.A.; Gutierrez, L.; Weiss, A.; Leichtmann-Bardoogo, Y.; Zhang, D.L.; Crooks, D.R.; Sougrat, R.; Morgenstern, A.; Galy, B.; Hentze, M.W.; et al. Serum ferritin is derived primarily from macrophages through a nonclassical secretory pathway. *Blood* **2010**, *116*, 1574–1584. [[CrossRef](#)]
101. Sun, Q.; Yang, F.; Wang, H.; Cui, F.; Li, Y.; Li, S.; Ren, Y.; Lan, W.; Li, M.; Zhu, W.; et al. Elevated serum ferritin level as a predictor of reduced survival in patients with sporadic amyotrophic lateral sclerosis in China: A retrospective study. *Amyotroph. Lateral Scler. Front. Degener.* **2019**, *20*, 186–191. [[CrossRef](#)] [[PubMed](#)]
102. Li, R.; Luo, C.; Mines, M.; Zhang, J.; Fan, G.H. Chemokine CXCL12 induces binding of ferritin heavy chain to the chemokine receptor CXCR4, alters CXCR4 signaling, and induces phosphorylation and nuclear translocation of ferritin heavy chain. *J. Biol. Chem.* **2006**, *281*, 37616–37627. [[CrossRef](#)]
103. Fisher, J.; Devraj, K.; Ingram, J.; Slagle-Webb, B.; Madhankumar, A.B.; Liu, X.; Klinger, M.; Simpson, I.A.; Connor, J.R. Ferritin: A novel mechanism for delivery of iron to the brain and other organs. *Am. J. Physiol. Cell Physiol.* **2007**, *293*, C641–C649. [[CrossRef](#)] [[PubMed](#)]
104. Chiou, B.; Neal, E.H.; Bowman, A.B.; Lippmann, E.S.; Simpson, I.A.; Connor, J.R. Endothelial cells are critical regulators of iron transport in a model of the human blood-brain barrier. *J. Cereb. Blood Flow Metab.* **2019**, *39*, 2117–2131. [[CrossRef](#)]
105. Chiou, B.; Connor, J.R. Emerging and Dynamic Biomedical Uses of Ferritin. *Pharmaceuticals* **2018**, *11*, 124. [[CrossRef](#)] [[PubMed](#)]
106. Li, J.Y.; Paragas, N.; Ned, R.M.; Qiu, A.; Viltard, M.; Leete, T.; Drexler, I.R.; Chen, X.; Sanna-Cherchi, S.; Mohammed, F.; et al. Scara5 is a ferritin receptor mediating non-transferrin iron delivery. *Dev. Cell* **2009**, *16*, 35–46. [[CrossRef](#)] [[PubMed](#)]
107. Li, L.; Fang, C.J.; Ryan, J.C.; Niemi, E.C.; Lebron, J.A.; Bjorkman, P.J.; Arase, H.; Torti, F.M.; Torti, S.V.; Nakamura, M.C.; et al. Binding and uptake of H-ferritin are mediated by human transferrin receptor-1. *Proc. Natl. Acad. Sci. USA* **2010**, *107*, 3505–3510. [[CrossRef](#)] [[PubMed](#)]
108. Wang, X.S.; Ong, W.Y.; Connor, J.R. A light and electron microscopic study of the iron transporter protein DMT-1 in the monkey cerebral neocortex and hippocampus. *J. Neurocytol.* **2001**, *30*, 353–360. [[CrossRef](#)] [[PubMed](#)]
109. Dringen, R.; Bishop, G.M.; Koeppe, M.; Dang, T.N.; Robinson, S.R. The pivotal role of astrocytes in the metabolism of iron in the brain. *Neurochem. Res.* **2007**, *32*, 1884–1890. [[CrossRef](#)] [[PubMed](#)]
110. Moos, T.; Morgan, E.H. Evidence for low molecular weight, non-transferrin-bound iron in rat brain and cerebrospinal fluid. *J. Neurosci. Res.* **1998**, *54*, 486–494. [[CrossRef](#)]
111. Gilbert, B.C. *Free Radicals and Iron: Chemistry, Biology and Medicine*; Symons, M.C.R., Gutteridge, J.M.C., Eds.; Oxford University Press: Oxford, UK, 1998; ISBN 0-19-855892-9.
112. Moos, T.; Rosengren Nielsen, T.; Skjorringe, T.; Morgan, E.H. Iron trafficking inside the brain. *J. Neurochem.* **2007**, *103*, 1730–1740. [[CrossRef](#)] [[PubMed](#)]
113. Ganz, T. Heparin—a regulator of intestinal iron absorption and iron recycling by macrophages. *Best Pract. Res. Clin. Haematol.* **2005**, *18*, 171–182. [[CrossRef](#)] [[PubMed](#)]
114. Brasse-Lagnel, C.; Karim, Z.; Letteron, P.; Bekri, S.; Bado, A.; Beaumont, C. Intestinal DMT1 cotransporter is down-regulated by hepcidin via proteasome internalization and degradation. *Gastroenterology* **2011**, *140*, 1261–1271.e1261. [[CrossRef](#)] [[PubMed](#)]
115. Mena, N.P.; Esparza, A.; Tapia, V.; Valdes, P.; Nunez, M.T. Heparin inhibits apical iron uptake in intestinal cells. *Am. J. Physiol. Gastrointest. Liver Physiol.* **2008**, *294*, G192–G198. [[CrossRef](#)] [[PubMed](#)]
116. Nemeth, E.; Tuttle, M.S.; Powelson, J.; Vaughn, M.B.; Donovan, A.; Ward, D.M.; Ganz, T.; Kaplan, J. Heparin regulates cellular iron efflux by binding to ferroportin and inducing its internalization. *Science* **2004**, *306*, 2090–2093. [[CrossRef](#)] [[PubMed](#)]
117. Billesbolle, C.B.; Azumaya, C.M.; Kretsch, R.C.; Powers, A.S.; Gonen, S.; Schneider, S.; Arvedson, T.; Dror, R.O.; Cheng, Y.; Manglik, A. Structure of hepcidin-bound ferroportin reveals iron homeostatic mechanisms. *Nature* **2020**, *586*, 807–811. [[CrossRef](#)] [[PubMed](#)]
118. Enns, C.A.; Ahmed, R.; Wang, J.; Ueno, A.; Worthen, C.; Tsukamoto, H.; Zhang, A.S. Increased iron loading induces Bmp6 expression in the non-parenchymal cells of the liver independent of the BMP-signaling pathway. *PLoS ONE* **2013**, *8*, e60534. [[CrossRef](#)]

119. Babbitt, J.L.; Huang, F.W.; Xia, Y.; Sidis, Y.; Andrews, N.C.; Lin, H.Y. Modulation of bone morphogenetic protein signaling in vivo regulates systemic iron balance. *J. Clin. Investig.* **2007**, *117*, 1933–1939. [[CrossRef](#)]
120. Truksa, J.; Peng, H.; Lee, P.; Beutler, E. Bone morphogenetic proteins 2, 4, and 9 stimulate murine hepcidin 1 expression independently of Hfe, transferrin receptor 2 (Tfr2), and IL-6. *Proc. Natl. Acad. Sci. USA* **2006**, *103*, 10289–10293. [[CrossRef](#)]
121. Robb, A.; Wessling-Resnick, M. Regulation of transferrin receptor 2 protein levels by transferrin. *Blood* **2004**, *104*, 4294–4299. [[CrossRef](#)]
122. Goswami, T.; Andrews, N.C. Hereditary hemochromatosis protein, HFE, interaction with transferrin receptor 2 suggests a molecular mechanism for mammalian iron sensing. *J. Biol. Chem.* **2006**, *281*, 28494–28498. [[CrossRef](#)] [[PubMed](#)]
123. Wrighting, D.M.; Andrews, N.C. Interleukin-6 induces hepcidin expression through STAT3. *Blood* **2006**, *108*, 3204–3209. [[CrossRef](#)]
124. Wallace, D.F.; Subramaniam, V.N. Analysis of IL-22 contribution to hepcidin induction and hypoferrremia during the response to LPS in vivo. *Int. Immunol.* **2015**, *27*, 281–287. [[CrossRef](#)]
125. Kanamori, Y.; Murakami, M.; Sugiyama, M.; Hashimoto, O.; Matsui, T.; Funaba, M. Interleukin-1beta (IL-1beta) transcriptionally activates hepcidin by inducing CCAAT enhancer-binding protein delta (C/EBPdelta) expression in hepatocytes. *J. Biol. Chem.* **2017**, *292*, 10275–10287. [[CrossRef](#)] [[PubMed](#)]
126. Wang, R.H.; Li, C.; Xu, X.; Zheng, Y.; Xiao, C.; Zervas, P.; Cooperman, S.; Eckhaus, M.; Rouault, T.; Mishra, L.; et al. A role of SMAD4 in iron metabolism through the positive regulation of hepcidin expression. *Cell Metab.* **2005**, *2*, 399–409. [[CrossRef](#)] [[PubMed](#)]
127. Kautz, L.; Jung, G.; Valore, E.V.; Rivella, S.; Nemeth, E.; Ganz, T. Identification of erythroferrone as an erythroid regulator of iron metabolism. *Nat. Genet.* **2014**, *46*, 678–684. [[CrossRef](#)]
128. Ganz, T. Erythropoietic regulators of iron metabolism. *Free Radic. Biol. Med.* **2019**, *133*, 69–74. [[CrossRef](#)]
129. Wang, C.Y.; Core, A.B.; Canali, S.; Zumbrennen-Bullough, K.B.; Ozer, S.; Umans, L.; Zwijsen, A.; Babbitt, J.L. Smad1/5 is required for erythropoietin-mediated suppression of hepcidin in mice. *Blood* **2017**, *130*, 73–83. [[CrossRef](#)] [[PubMed](#)]
130. Zechel, S.; Huber-Wittmer, K.; von Bohlen und Halbach, O. Distribution of the iron-regulating protein hepcidin in the murine central nervous system. *J. Neurosci. Res.* **2006**, *84*, 790–800. [[CrossRef](#)]
131. Wang, S.M.; Fu, L.J.; Duan, X.L.; Crooks, D.R.; Yu, P.; Qian, Z.M.; Di, X.J.; Li, J.; Rouault, T.A.; Chang, Y.Z. Role of hepcidin in murine brain iron metabolism. *Cell Mol. Life Sci.* **2010**, *67*, 123–133. [[CrossRef](#)]
132. Hanninen, M.M.; Haapasalo, J.; Haapasalo, H.; Fleming, R.E.; Britton, R.S.; Bacon, B.R.; Parkkila, S. Expression of iron-related genes in human brain and brain tumors. *BMC Neurosci.* **2009**, *10*, 36. [[CrossRef](#)]
133. Yanase, K.; Uemura, N.; Chiba, Y.; Murakami, R.; Fujihara, R.; Matsumoto, K.; Shirakami, G.; Araki, N.; Ueno, M. Immunoreactivities for hepcidin, ferroportin, and hephaestin in astrocytes and choroid plexus epithelium of human brains. *Neuropathology* **2020**, *40*, 75–83. [[CrossRef](#)] [[PubMed](#)]
134. Lu, L.N.; Qian, Z.M.; Wu, K.C.; Yung, W.H.; Ke, Y. Expression of Iron Transporters and Pathological Hallmarks of Parkinson's and Alzheimer's Diseases in the Brain of Young, Adult, and Aged Rats. *Mol. Neurobiol.* **2017**, *54*, 5213–5224. [[CrossRef](#)] [[PubMed](#)]
135. Raha-Chowdhury, R.; Raha, A.A.; Forostyak, S.; Zhao, J.W.; Stott, S.R.; Bomford, A. Expression and cellular localization of hepcidin mRNA and protein in normal rat brain. *BMC Neurosci.* **2015**, *16*, 24. [[CrossRef](#)] [[PubMed](#)]
136. Vela, D. Hepcidin, an emerging and important player in brain iron homeostasis. *J. Transl. Med.* **2018**, *16*, 25. [[CrossRef](#)] [[PubMed](#)]
137. Urrutia, P.; Aguirre, P.; Esparza, A.; Tapia, V.; Mena, N.P.; Arredondo, M.; Gonzalez-Billault, C.; Nunez, M.T. Inflammation alters the expression of DMT1, FPN1 and hepcidin, and it causes iron accumulation in central nervous system cells. *J. Neurochem.* **2013**, *126*, 541–549. [[CrossRef](#)]
138. Burkhardt, A.; Skjorringe, T.; Johnsen, K.B.; Siupka, P.; Thomsen, L.B.; Nielsen, M.S.; Thomsen, L.L.; Moos, T. Expression of Iron-Related Proteins at the Neurovascular Unit Supports Reduction and Reoxidation of Iron for Transport Through the Blood-Brain Barrier. *Mol. Neurobiol.* **2016**, *53*, 7237–7253. [[CrossRef](#)]
139. Hadziahmetovic, M.; Song, Y.; Ponnuru, P.; Iacovelli, J.; Hunter, A.; Haddad, N.; Beard, J.; Connor, J.R.; Vaulont, S.; Dunaief, J.L. Age-dependent retinal iron accumulation and degeneration in hepcidin knockout mice. *Investig. Ophthalmol. Vis. Sci.* **2011**, *52*, 109–118. [[CrossRef](#)]
140. McCarthy, R.C.; Kosman, D.J. Glial cell ceruloplasmin and hepcidin differentially regulate iron efflux from brain microvascular endothelial cells. *PLoS ONE* **2014**, *9*, e89003. [[CrossRef](#)]
141. Simpson, I.A.; Ponnuru, P.; Klinger, M.E.; Myers, R.L.; Devraj, K.; Coe, C.L.; Lubach, G.R.; Carruthers, A.; Connor, J.R. A novel model for brain iron uptake: Introducing the concept of regulation. *J. Cereb. Blood Flow Metab.* **2015**, *35*, 48–57. [[CrossRef](#)]
142. Malik, I.A.; Naz, N.; Sheikh, N.; Khan, S.; Moriconi, F.; Blaschke, M.; Ramadori, G. Comparison of changes in gene expression of transferrin receptor-1 and other iron-regulatory proteins in rat liver and brain during acute-phase response. *Cell Tissue Res.* **2011**, *344*, 299–312. [[CrossRef](#)] [[PubMed](#)]
143. Qian, Z.M.; He, X.; Liang, T.; Wu, K.C.; Yan, Y.C.; Lu, L.N.; Yang, G.; Luo, Q.Q.; Yung, W.H.; Ke, Y. Lipopolysaccharides upregulate hepcidin in neuron via microglia and the IL-6/STAT3 signaling pathway. *Mol. Neurobiol.* **2014**, *50*, 811–820. [[CrossRef](#)] [[PubMed](#)]
144. Zhang, F.L.; Hou, H.M.; Yin, Z.N.; Chang, L.; Li, F.M.; Chen, Y.J.; Ke, Y.; Qian, Z.M. Impairment of Hepcidin Upregulation by Lipopolysaccharide in the Interleukin-6 Knockout Mouse Brain. *Front. Mol. Neurosci.* **2017**, *10*, 367. [[CrossRef](#)] [[PubMed](#)]
145. Wang, Q.; Du, F.; Qian, Z.M.; Ge, X.H.; Zhu, L.; Yung, W.H.; Yang, L.; Ke, Y. Lipopolysaccharide induces a significant increase in expression of iron regulatory hormone hepcidin in the cortex and substantia nigra in rat brain. *Endocrinology* **2008**, *149*, 3920–3925. [[CrossRef](#)] [[PubMed](#)]

146. Marques, F.; Falcao, A.M.; Sousa, J.C.; Coppola, G.; Geschwind, D.; Sousa, N.; Correia-Neves, M.; Palha, J.A. Altered iron metabolism is part of the choroid plexus response to peripheral inflammation. *Endocrinology* **2009**, *150*, 2822–2828. [[CrossRef](#)]
147. Ma, J.; Zhang, F.L.; Zhou, G.; Bao, Y.X.; Shen, Y.; Qian, Z.M. Different Characteristics of Hepcidin Expression in IL-6+/+ and IL-6-/- Neurons and Astrocytes Treated with Lipopolysaccharides. *Neurochem. Res.* **2018**, *43*, 1624–1630. [[CrossRef](#)]
148. You, L.H.; Yan, C.Z.; Zheng, B.J.; Ci, Y.Z.; Chang, S.Y.; Yu, P.; Gao, G.F.; Li, H.Y.; Dong, T.Y.; Chang, Y.Z. Astrocyte hepcidin is a key factor in LPS-induced neuronal apoptosis. *Cell Death Dis.* **2017**, *8*, e2676. [[CrossRef](#)]
149. Du, F.; Qian, Z.M.; Luo, Q.; Yung, W.H.; Ke, Y. Hepcidin Suppresses Brain Iron Accumulation by Downregulating Iron Transport Proteins in Iron-Overloaded Rats. *Mol. Neurobiol.* **2015**, *52*, 101–114. [[CrossRef](#)]
150. Xu, Q.; Kanthasamy, A.G.; Jin, H.; Reddy, M.B. Hepcidin Plays a Key Role in 6-OHDA Induced Iron Overload and Apoptotic Cell Death in a Cell Culture Model of Parkinson's Disease. *Park. Dis.* **2016**, *2016*, 8684130. [[CrossRef](#)]
151. Gong, J.; Du, F.; Qian, Z.M.; Luo, Q.Q.; Sheng, Y.; Yung, W.H.; Xu, Y.X.; Ke, Y. Pre-treatment of rats with ad-hepcidin prevents iron-induced oxidative stress in the brain. *Free Radic. Biol. Med.* **2016**, *90*, 126–132. [[CrossRef](#)]
152. Liang, T.; Qian, Z.M.; Mu, M.D.; Yung, W.H.; Ke, Y. Brain Hepcidin Suppresses Major Pathologies in Experimental Parkinsonism. *iScience* **2020**, *23*, 101284. [[CrossRef](#)] [[PubMed](#)]
153. Li, M.; Hu, J.; Yuan, X.; Shen, L.; Zhu, L.; Luo, Q. Hepcidin Decreases Rotenone-Induced alpha-Synuclein Accumulation via Autophagy in SH-SY5Y Cells. *Front. Mol. Neurosci.* **2020**, *13*, 560891. [[CrossRef](#)]
154. Urrutia, P.J.; Hirsch, E.C.; Gonzalez-Billault, C.; Nunez, M.T. Hepcidin attenuates amyloid beta-induced inflammatory and pro-oxidant responses in astrocytes and microglia. *J. Neurochem.* **2017**, *142*, 140–152. [[CrossRef](#)] [[PubMed](#)]
155. Xu, Y.; Zhang, Y.; Zhang, J.H.; Han, K.; Zhang, X.; Bai, X.; You, L.H.; Yu, P.; Shi, Z.; Chang, Y.Z.; et al. Astrocyte hepcidin ameliorates neuronal loss through attenuating brain iron deposition and oxidative stress in APP/PS1 mice. *Free Radic. Biol. Med.* **2020**, *158*, 84–95. [[CrossRef](#)] [[PubMed](#)]
156. Raha, A.A.; Vaishnav, R.A.; Friedland, R.P.; Bomford, A.; Raha-Chowdhury, R. The systemic iron-regulatory proteins hepcidin and ferroportin are reduced in the brain in Alzheimer's disease. *Acta Neuropathol. Commun.* **2013**, *1*, 55. [[CrossRef](#)] [[PubMed](#)]
157. Wilkinson, N.; Pantopoulos, K. The IRP/IRE system in vivo: Insights from mouse models. *Front. Pharmacol.* **2014**, *5*, 176. [[CrossRef](#)] [[PubMed](#)]
158. Pantopoulos, K. Iron metabolism and the IRE/IRP regulatory system: An update. *Ann. N. Y. Acad. Sci.* **2004**, *1012*, 1–13. [[CrossRef](#)] [[PubMed](#)]
159. Piccinelli, P.; Samuelsson, T. Evolution of the iron-responsive element. *RNA* **2007**, *13*, 952–966. [[CrossRef](#)]
160. Maione, V.; Cantini, F.; Severi, M.; Banci, L. Investigating the role of the human CIA2A-CIAO1 complex in the maturation of aconitase. *Biochim. Biophys. Acta Gen. Subj.* **2018**, *1862*, 1980–1987. [[CrossRef](#)]
161. Stehling, O.; Mascarenhas, J.; Vashisht, A.A.; Sheftel, A.D.; Niggemeyer, B.; Rosser, R.; Pierik, A.J.; Wohlschlegel, J.A.; Lill, R. Human CIA2A-FAM96A and CIA2B-FAM96B integrate iron homeostasis and maturation of different subsets of cytosolic-nuclear iron-sulfur proteins. *Cell Metab.* **2013**, *18*, 187–198. [[CrossRef](#)]
162. Martelli, A.; Schmucker, S.; Reutenauer, L.; Mathieu, J.R.R.; Peyssonnaud, C.; Karim, Z.; Puy, H.; Galy, B.; Hentze, M.W.; Puccio, H. Iron regulatory protein 1 sustains mitochondrial iron loading and function in frataxin deficiency. *Cell Metab.* **2015**, *21*, 311–323. [[CrossRef](#)]
163. Galy, B.; Ferring-Appel, D.; Sauer, S.W.; Kaden, S.; Lyoumi, S.; Puy, H.; Kolker, S.; Grone, H.J.; Hentze, M.W. Iron regulatory proteins secure mitochondrial iron sufficiency and function. *Cell Metab.* **2010**, *12*, 194–201. [[CrossRef](#)] [[PubMed](#)]
164. Lee, D.W.; Kaur, D.; Chinta, S.J.; Rajagopalan, S.; Andersen, J.K. A disruption in iron-sulfur center biogenesis via inhibition of mitochondrial dithiol glutaredoxin 2 may contribute to mitochondrial and cellular iron dysregulation in mammalian glutathione-depleted dopaminergic cells: Implications for Parkinson's disease. *Antioxid. Redox. Signal.* **2009**, *11*, 2083–2094. [[CrossRef](#)] [[PubMed](#)]
165. Ye, H.; Jeong, S.Y.; Ghosh, M.C.; Kovtunovych, G.; Silvestri, L.; Ortillo, D.; Uchida, N.; Tisdale, J.; Camaschella, C.; Rouault, T.A. Glutaredoxin 5 deficiency causes sideroblastic anemia by specifically impairing heme biosynthesis and depleting cytosolic iron in human erythroblasts. *J. Clin. Investig.* **2010**, *120*, 1749–1761. [[CrossRef](#)] [[PubMed](#)]
166. Paul, B.T.; Tesfay, L.; Winkler, C.R.; Torti, F.M.; Torti, S.V. Sideroflexin 4 affects Fe-S cluster biogenesis, iron metabolism, mitochondrial respiration and heme biosynthetic enzymes. *Sci. Rep.* **2019**, *9*, 19634. [[CrossRef](#)] [[PubMed](#)]
167. Wu, H.; Wei, H.; Zhang, D.; Sehgal, S.A.; Zhang, D.; Wang, X.; Qin, Y.; Liu, L.; Chen, Q. Defective mitochondrial ISCs biogenesis switches on IRP1 to fine tune selective mitophagy. *Redox. Biol.* **2020**, *36*, 101661. [[CrossRef](#)] [[PubMed](#)]
168. Allen, G.F.; Toth, R.; James, J.; Ganley, I.G. Loss of iron triggers PINK1/Parkin-independent mitophagy. *EMBO Rep.* **2013**, *14*, 1127–1135. [[CrossRef](#)]
169. Chung, J.; Anderson, S.A.; Gwynn, B.; Deck, K.M.; Chen, M.J.; Langer, N.B.; Shaw, G.C.; Huston, N.C.; Boyer, L.F.; Datta, S.; et al. Iron regulatory protein-1 protects against mitoferrin-1-deficient porphyria. *J. Biol. Chem.* **2014**, *289*, 7835–7843. [[CrossRef](#)]
170. Ogura, M.; Endo, R.; Ishikawa, H.; Takeda, Y.; Uchida, T.; Iwai, K.; Kobayashi, K.; Ishimori, K. Redox-dependent axial ligand replacement and its functional significance in heme-bound iron regulatory proteins. *J. Inorg. Biochem.* **2018**, *182*, 238–248. [[CrossRef](#)]
171. Nishitani, Y.; Okutani, H.; Takeda, Y.; Uchida, T.; Iwai, K.; Ishimori, K. Specific heme binding to heme regulatory motifs in iron regulatory proteins and its functional significance. *J. Inorg. Biochem.* **2019**, *198*, 110726. [[CrossRef](#)]

172. Salahudeen, A.A.; Thompson, J.W.; Ruiz, J.C.; Ma, H.W.; Kinch, L.N.; Li, Q.; Grishin, N.V.; Bruick, R.K. An E3 ligase possessing an iron-responsive hemerythrin domain is a regulator of iron homeostasis. *Science* **2009**, *326*, 722–726. [[CrossRef](#)] [[PubMed](#)]
173. Vashisht, A.A.; Zumbrennen, K.B.; Huang, X.; Powers, D.N.; Durazo, A.; Sun, D.; Bhaskaran, N.; Persson, A.; Uhlen, M.; Sangfelt, O.; et al. Control of iron homeostasis by an iron-regulated ubiquitin ligase. *Science* **2009**, *326*, 718–721. [[CrossRef](#)]
174. Thompson, J.W.; Salahudeen, A.A.; Chollangi, S.; Ruiz, J.C.; Brautigam, C.A.; Makris, T.M.; Lipscomb, J.D.; Tomchick, D.R.; Bruick, R.K. Structural and molecular characterization of iron-sensing hemerythrin-like domain within F-box and leucine-rich repeat protein 5 (FBXL5). *J. Biol. Chem.* **2012**, *287*, 7357–7365. [[CrossRef](#)] [[PubMed](#)]
175. Moroishi, T.; Yamauchi, T.; Nishiyama, M.; Nakayama, K.I. HERC2 targets the iron regulator FBXL5 for degradation and modulates iron metabolism. *J. Biol. Chem.* **2014**, *289*, 16430–16441. [[CrossRef](#)] [[PubMed](#)]
176. Wang, H.; Shi, H.; Rajan, M.; Canarie, E.R.; Hong, S.; Simoneschi, D.; Pagano, M.; Bush, M.F.; Stoll, S.; Leibold, E.A.; et al. FBXL5 Regulates IRP2 Stability in Iron Homeostasis via an Oxygen-Responsive [2Fe2S] Cluster. *Mol. Cell.* **2020**, *78*, 31–41.e35. [[CrossRef](#)] [[PubMed](#)]
177. Mayank, A.K.; Pandey, V.; Vashisht, A.A.; Barshop, W.D.; Rayatpisheh, S.; Sharma, T.; Haque, T.; Powers, D.N.; Wohlschlegel, J.A. An Oxygen-Dependent Interaction between FBXL5 and the CIA-Targeting Complex Regulates Iron Homeostasis. *Mol. Cell.* **2019**, *75*, 382–393. [[CrossRef](#)] [[PubMed](#)]
178. Wilkinson, N.; Pantopoulos, K. IRP1 regulates erythropoiesis and systemic iron homeostasis by controlling HIF2alpha mRNA translation. *Blood* **2013**, *122*, 1658–1668. [[CrossRef](#)]
179. Anderson, S.A.; Nizzi, C.P.; Chang, Y.I.; Deck, K.M.; Schmidt, P.J.; Galy, B.; Damnernasawad, A.; Broman, A.T.; Kendzierski, C.; Hentze, M.W.; et al. The IRP1-HIF-2alpha axis coordinates iron and oxygen sensing with erythropoiesis and iron absorption. *Cell. Metab.* **2013**, *17*, 282–290. [[CrossRef](#)]
180. LaVaute, T.; Smith, S.; Cooperman, S.; Iwai, K.; Land, W.; Meyron-Holtz, E.; Drake, S.K.; Miller, G.; Abu-Asab, M.; Tsokos, M.; et al. Targeted deletion of the gene encoding iron regulatory protein-2 causes misregulation of iron metabolism and neurodegenerative disease in mice. *Nat. Genet.* **2001**, *27*, 209–214. [[CrossRef](#)]
181. Meyron-Holtz, E.G.; Ghosh, M.C.; Iwai, K.; LaVaute, T.; Brazzolotto, X.; Berger, U.V.; Land, W.; Ollivierre-Wilson, H.; Grinberg, A.; Love, P.; et al. Genetic ablations of iron regulatory proteins 1 and 2 reveal why iron regulatory protein 2 dominates iron homeostasis. *EMBO J.* **2004**, *23*, 386–395. [[CrossRef](#)]
182. Ruiz, J.C.; Walker, S.D.; Anderson, S.A.; Eisenstein, R.S.; Bruick, R.K. F-box and leucine-rich repeat protein 5 (FBXL5) is required for maintenance of cellular and systemic iron homeostasis. *J. Biol. Chem.* **2013**, *288*, 552–560. [[CrossRef](#)] [[PubMed](#)]
183. Moroishi, T.; Nishiyama, M.; Takeda, Y.; Iwai, K.; Nakayama, K.I. The FBXL5-IRP2 axis is integral to control of iron metabolism in vivo. *Cell Metab.* **2011**, *14*, 339–351. [[CrossRef](#)] [[PubMed](#)]
184. Meyron-Holtz, E.G.; Ghosh, M.C.; Rouault, T.A. Mammalian tissue oxygen levels modulate iron-regulatory protein activities in vivo. *Science* **2004**, *306*, 2087–2090. [[CrossRef](#)] [[PubMed](#)]
185. Ghosh, M.C.; Tong, W.H.; Zhang, D.; Ollivierre-Wilson, H.; Singh, A.; Krishna, M.C.; Mitchell, J.B.; Rouault, T.A. Tempol-mediated activation of latent iron regulatory protein activity prevents symptoms of neurodegenerative disease in IRP2 knockout mice. *Proc. Natl. Acad. Sci. USA* **2008**, *105*, 12028–12033. [[CrossRef](#)]
186. Missirlis, F.; Hu, J.; Kirby, K.; Hilliker, A.J.; Rouault, T.A.; Phillips, J.P. Compartment-specific protection of iron-sulfur proteins by superoxide dismutase. *J. Biol. Chem.* **2003**, *278*, 47365–47369. [[CrossRef](#)]
187. Starzynski, R.R.; Lipinski, P.; Drapier, J.C.; Diet, A.; Smuda, E.; Bartłomieńczyk, T.; Gralak, M.A.; Kruszewski, M. Down-regulation of iron regulatory protein 1 activities and expression in superoxide dismutase 1 knock-out mice is not associated with alterations in iron metabolism. *J. Biol. Chem.* **2005**, *280*, 4207–4212. [[CrossRef](#)]
188. Milczarek, A.; Starzynski, R.R.; Stys, A.; Jonczy, A.; Staron, R.; Grzelak, A.; Lipinski, P. A drastic superoxide-dependent oxidative stress is prerequisite for the down-regulation of IRP1: Insights from studies on SOD1-deficient mice and macrophages treated with paraquat. *PLoS ONE* **2017**, *12*, e0176800. [[CrossRef](#)]
189. Johnson, N.B.; Deck, K.M.; Nizzi, C.P.; Eisenstein, R.S. A synergistic role of IRP1 and FBXL5 proteins in coordinating iron metabolism during cell proliferation. *J. Biol. Chem.* **2017**, *292*, 15976–15989. [[CrossRef](#)]
190. Sureda, A.; Hebling, U.; Pons, A.; Mueller, S. Extracellular H₂O₂ and not superoxide determines the compartment-specific activation of transferrin receptor by iron regulatory protein 1. *Free Radic. Res.* **2005**, *39*, 817–824. [[CrossRef](#)]
191. Brazzolotto, X.; Gaillard, J.; Pantopoulos, K.; Hentze, M.W.; Moulis, J.M. Human cytoplasmic aconitase (Iron regulatory protein 1) is converted into its [3Fe-4S] form by hydrogen peroxide in vitro but is not activated for iron-responsive element binding. *J. Biol. Chem.* **1999**, *274*, 21625–21630. [[CrossRef](#)]
192. Pantopoulos, K.; Mueller, S.; Atzberger, A.; Ansorge, W.; Stremmel, W.; Hentze, M.W. Differences in the regulation of iron regulatory protein-1 (IRP-1) by extra- and intracellular oxidative stress. *J. Biol. Chem.* **1997**, *272*, 9802–9808. [[CrossRef](#)] [[PubMed](#)]
193. Pantopoulos, K.; Hentze, M.W. Activation of iron regulatory protein-1 by oxidative stress in vitro. *Proc. Natl. Acad. Sci. USA* **1998**, *95*, 10559–10563. [[CrossRef](#)] [[PubMed](#)]
194. Pantopoulos, K.; Hentze, M.W. Rapid responses to oxidative stress mediated by iron regulatory protein. *EMBO J.* **1995**, *14*, 2917–2924. [[CrossRef](#)] [[PubMed](#)]
195. Dev, S.; Kumari, S.; Singh, N.; Kumar Bal, S.; Seth, P.; Mukhopadhyay, C.K. Role of extracellular Hydrogen peroxide in regulation of iron homeostasis genes in neuronal cells: Implication in iron accumulation. *Free Radic. Biol. Med.* **2015**, *86*, 78–89. [[CrossRef](#)] [[PubMed](#)]

196. Soum, E.; Brazzolotto, X.; Goussias, C.; Bouton, C.; Moulis, J.M.; Mattioli, T.A.; Drapier, J.C. Peroxynitrite and nitric oxide differently target the iron-sulfur cluster and amino acid residues of human iron regulatory protein 1. *Biochemistry* **2003**, *42*, 7648–7654. [[CrossRef](#)]
197. Soum, E.; Drapier, J.C. Nitric oxide and peroxynitrite promote complete disruption of the [4Fe-4S] cluster of recombinant human iron regulatory protein 1. *J. Biol. Inorg. Chem.* **2003**, *8*, 226–232. [[CrossRef](#)]
198. Lipinski, P.; Starzynski, R.R.; Drapier, J.C.; Bouton, C.; Bartlomiejczyk, T.; Sochanowicz, B.; Smuda, E.; Gajkowska, A.; Kruszewski, M. Induction of iron regulatory protein 1 RNA-binding activity by nitric oxide is associated with a concomitant increase in the labile iron pool: Implications for DNA damage. *Biochem. Biophys. Res. Commun.* **2005**, *327*, 349–355. [[CrossRef](#)]
199. Phillips, J.D.; Kinikini, D.V.; Yu, Y.; Guo, B.; Leibold, E.A. Differential regulation of IRP1 and IRP2 by nitric oxide in rat hepatoma cells. *Blood* **1996**, *87*, 2983–2992. [[CrossRef](#)]
200. Stys, A.; Galy, B.; Starzynski, R.R.; Smuda, E.; Drapier, J.C.; Lipinski, P.; Bouton, C. Iron regulatory protein 1 outcompetes iron regulatory protein 2 in regulating cellular iron homeostasis in response to nitric oxide. *J. Biol. Chem.* **2011**, *286*, 22846–22854. [[CrossRef](#)]
201. Oliveira, L.; Bouton, C.; Drapier, J.C. Thioredoxin activation of iron regulatory proteins. *J. Biol. Chem.* **1999**, *274*, 516–521. [[CrossRef](#)]
202. Gonzalez, D.; Drapier, J.C.; Bouton, C. Endogenous nitration of iron regulatory protein-1 (IRP-1) in nitric oxide-producing murine macrophages: Further insight into the mechanism of nitration in vivo and its impact on IRP-1 functions. *J. Biol. Chem.* **2004**, *279*, 43345–43351. [[CrossRef](#)] [[PubMed](#)]
203. Bouton, C.; Hirling, H.; Drapier, J.C. Redox modulation of iron regulatory proteins by peroxynitrite. *J. Biol. Chem.* **1997**, *272*, 19969–19975. [[CrossRef](#)] [[PubMed](#)]
204. Bouton, C.; Chauveau, M.J.; Lazereg, S.; Drapier, J.C. Recycling of RNA binding iron regulatory protein 1 into an aconitase after nitric oxide removal depends on mitochondrial ATP. *J. Biol. Chem.* **2002**, *277*, 31220–31227. [[CrossRef](#)] [[PubMed](#)]
205. Ferecatu, I.; Goncalves, S.; Golinelli-Cohen, M.P.; Clemancey, M.; Martelli, A.; Riquier, S.; Guittet, E.; Latour, J.M.; Puccio, H.; Drapier, J.C.; et al. The diabetes drug target MitoNEET governs a novel trafficking pathway to rebuild an Fe-S cluster into cytosolic aconitase/iron regulatory protein 1. *J. Biol. Chem.* **2014**, *289*, 28070–28086. [[CrossRef](#)] [[PubMed](#)]
206. Golinelli-Cohen, M.P.; Lescop, E.; Mons, C.; Goncalves, S.; Clemancey, M.; Santolini, J.; Guittet, E.; Blondin, G.; Latour, J.M.; Bouton, C. Redox Control of the Human Iron-Sulfur Repair Protein MitoNEET Activity via Its Iron-Sulfur Cluster. *J. Biol. Chem.* **2016**, *291*, 7583–7593. [[CrossRef](#)]
207. Geldenhuys, W.J.; Benkovic, S.A.; Lin, L.; Yonutas, H.M.; Crish, S.D.; Sullivan, P.G.; Darvesh, A.S.; Brown, C.M.; Richardson, J.R. MitoNEET (CISD1) Knockout Mice Show Signs of Striatal Mitochondrial Dysfunction and a Parkinson’s Disease Phenotype. *ACS Chem. Neurosci.* **2017**, *8*, 2759–2765. [[CrossRef](#)] [[PubMed](#)]
208. Nunez, M.T.; Nunez-Millacura, C.; Tapia, V.; Munoz, P.; Mazariegos, D.; Arredondo, M.; Munoz, P.; Mura, C.; Maccioni, R.B. Iron-activated iron uptake: A positive feedback loop mediated by iron regulatory protein 1. *Biomaterials* **2003**, *16*, 83–90. [[CrossRef](#)]
209. Nunez-Millacura, C.; Tapia, V.; Munoz, P.; Maccioni, R.B.; Nunez, M.T. An oxidative stress-mediated positive-feedback iron uptake loop in neuronal cells. *J. Neurochem.* **2002**, *82*, 240–248. [[CrossRef](#)]
210. Urrutia, P.J.; Aguirre, P.; Tapia, V.; Carrasco, C.M.; Mena, N.P.; Nunez, M.T. Cell death induced by mitochondrial complex I inhibition is mediated by Iron Regulatory Protein 1. *Biochim. Biophys. Acta Mol. Basis Dis.* **2017**, *1863*, 2202–2209. [[CrossRef](#)]
211. Mulero, V.; Brock, J.H. Regulation of iron metabolism in murine J774 macrophages: Role of nitric oxide-dependent and -independent pathways following activation with gamma interferon and lipopolysaccharide. *Blood* **1999**, *94*, 2383–2389. [[CrossRef](#)]
212. Thomsen, M.S.; Andersen, M.V.; Christoffersen, P.R.; Jensen, M.D.; Lichota, J.; Moos, T. Neurodegeneration with inflammation is accompanied by accumulation of iron and ferritin in microglia and neurons. *Neurobiol. Dis.* **2015**, *81*, 108–118. [[CrossRef](#)]
213. Wang, J.; Song, N.; Jiang, H.; Wang, J.; Xie, J. Pro-inflammatory cytokines modulate iron regulatory protein 1 expression and iron transportation through reactive oxygen/nitrogen species production in ventral mesencephalic neurons. *Biochim. Biophys. Acta Mol. Basis Dis.* **2013**, *1832*, 618–625. [[CrossRef](#)]
214. Faucheux, B.A.; Martin, M.E.; Beaumont, C.; Hunot, S.; Hauw, J.J.; Agid, Y.; Hirsch, E.C. Lack of up-regulation of ferritin is associated with sustained iron regulatory protein-1 binding activity in the substantia nigra of patients with Parkinson’s disease. *J. Neurochem.* **2002**, *83*, 320–330. [[CrossRef](#)]
215. Pinero, D.J.; Hu, J.; Connor, J.R. Alterations in the interaction between iron regulatory proteins and their iron responsive element in normal and Alzheimer’s diseased brains. *Cell Mol. Biol.* **2000**, *46*, 761–776.
216. Rogers, J.T.; Randall, J.D.; Cahill, C.M.; Eder, P.S.; Huang, X.; Gunshin, H.; Leiter, L.; McPhee, J.; Sarang, S.S.; Utsuki, T.; et al. An iron-responsive element type II in the 5′-untranslated region of the Alzheimer’s amyloid precursor protein transcript. *J. Biol. Chem.* **2002**, *277*, 45518–45528. [[CrossRef](#)]
217. Cho, H.H.; Cahill, C.M.; Vanderburg, C.R.; Scherzer, C.R.; Wang, B.; Huang, X.; Rogers, J.T. Selective translational control of the Alzheimer amyloid precursor protein transcript by iron regulatory protein-1. *J. Biol. Chem.* **2010**, *285*, 31217–31232. [[CrossRef](#)]
218. Duce, J.A.; Tsatsanis, A.; Cater, M.A.; James, S.A.; Robb, E.; Wikke, K.; Leong, S.L.; Perez, K.; Johanssen, T.; Greenough, M.A.; et al. Iron-export ferroxidase activity of beta-amyloid precursor protein is inhibited by zinc in Alzheimer’s disease. *Cell* **2010**, *142*, 857–867. [[CrossRef](#)]
219. Tsatsanis, A.; Dickens, S.; Kwok, J.C.F.; Wong, B.X.; Duce, J.A. Post Translational Modulation of beta-Amyloid Precursor Protein Trafficking to the Cell Surface Alters Neuronal Iron Homeostasis. *Neurochem. Res.* **2019**, *44*, 1367–1374. [[CrossRef](#)]

220. Tsatsanis, A.; Wong, B.X.; Gunn, A.P.; Ayton, S.; Bush, A.I.; Devos, D.; Duce, J.A. Amyloidogenic processing of Alzheimer's disease beta-amyloid precursor protein induces cellular iron retention. *Mol. Psychiatry* **2020**, *25*, 1958–1966. [[CrossRef](#)]
221. Wong, B.X.; Tsatsanis, A.; Lim, L.Q.; Adlard, P.A.; Bush, A.I.; Duce, J.A. beta-Amyloid precursor protein does not possess ferroxidase activity but does stabilize the cell surface ferrous iron exporter ferroportin. *PLoS ONE* **2014**, *9*, e114174. [[CrossRef](#)]
222. Ayton, S.; Lei, P.; Hare, D.J.; Duce, J.A.; George, J.L.; Adlard, P.A.; McLean, C.; Rogers, J.T.; Cherny, R.A.; Finkelstein, D.I.; et al. Parkinson's disease iron deposition caused by nitric oxide-induced loss of beta-amyloid precursor protein. *J. Neurosci.* **2015**, *35*, 3591–3597. [[CrossRef](#)]
223. Amici, S.A.; Dong, J.; Guerau-de-Arellano, M. Molecular Mechanisms Modulating the Phenotype of Macrophages and Microglia. *Front. Immunol.* **2017**, *8*, 1520. [[CrossRef](#)]
224. Corna, G.; Campana, L.; Pignatti, E.; Castiglioni, A.; Tagliafico, E.; Bosurgi, L.; Campanella, A.; Brunelli, S.; Manfredi, A.A.; Apostoli, P.; et al. Polarization dictates iron handling by inflammatory and alternatively activated macrophages. *Haematologica* **2010**, *95*, 1814–1822. [[CrossRef](#)]
225. Bouton, C.; Oliveira, L.; Drapier, J.C. Converse modulation of IRP1 and IRP2 by immunological stimuli in murine RAW 264.7 macrophages. *J. Biol. Chem.* **1998**, *273*, 9403–9408. [[CrossRef](#)]
226. Chenais, B.; Morjani, H.; Drapier, J.C. Impact of endogenous nitric oxide on microglial cell energy metabolism and labile iron pool. *J. Neurochem.* **2002**, *81*, 615–623. [[CrossRef](#)]
227. Recalcati, S.; Taramelli, D.; Conte, D.; Cairo, G. Nitric oxide-mediated induction of ferritin synthesis in J774 macrophages by inflammatory cytokines: Role of selective iron regulatory protein-2 downregulation. *Blood* **1998**, *91*, 1059–1066. [[CrossRef](#)]
228. Kim, S.; Ponka, P. Effects of interferon-gamma and lipopolysaccharide on macrophage iron metabolism are mediated by nitric oxide-induced degradation of iron regulatory protein 2. *J. Biol. Chem.* **2000**, *275*, 6220–6226. [[CrossRef](#)]
229. Kim, S.; Ponka, P. Control of transferrin receptor expression via nitric oxide-mediated modulation of iron-regulatory protein 2. *J. Biol. Chem.* **1999**, *274*, 33035–33042. [[CrossRef](#)]
230. Kim, S.; Ponka, P. Nitrogen monoxide-mediated control of ferritin synthesis: Implications for macrophage iron homeostasis. *Proc. Natl. Acad. Sci. USA* **2002**, *99*, 12214–12219. [[CrossRef](#)]
231. Reis, K.; Halldin, J.; Fernaeus, S.; Pettersson, C.; Land, T. NADPH oxidase inhibitor diphenyliodonium abolishes lipopolysaccharide-induced down-regulation of transferrin receptor expression in N2a and BV-2 cells. *J. Neurosci. Res.* **2006**, *84*, 1047–1052. [[CrossRef](#)]
232. McCarthy, R.C.; Sosa, J.C.; Gardeck, A.M.; Baez, A.S.; Lee, C.H.; Wessling-Resnick, M. Inflammation-induced iron transport and metabolism by brain microglia. *J. Biol. Chem.* **2018**, *293*, 7853–7863. [[CrossRef](#)]
233. Wardrop, S.L.; Richardson, D.R. Interferon-gamma and lipopolysaccharide regulate the expression of Nramp2 and increase the uptake of iron from low relative molecular mass complexes by macrophages. *Eur. J. Biochem.* **2000**, *267*, 6586–6593. [[CrossRef](#)]
234. Liu, X.B.; Hill, P.; Haile, D.J. Role of the ferroportin iron-responsive element in iron and nitric oxide dependent gene regulation. *Blood Cells Mol. Dis.* **2002**, *29*, 315–326. [[CrossRef](#)]
235. Oliveira, L.; Drapier, J.C. Down-regulation of iron regulatory protein 1 gene expression by nitric oxide. *Proc. Natl. Acad. Sci. USA* **2000**, *97*, 6550–6555. [[CrossRef](#)]
236. Zhou, Y.; Que, K.T.; Zhang, Z.; Yi, Z.J.; Zhao, P.X.; You, Y.; Gong, J.P.; Liu, Z.J. Iron overloaded polarizes macrophage to proinflammation phenotype through ROS/acetyl-p53 pathway. *Cancer Med.* **2018**, *7*, 4012–4022. [[CrossRef](#)]
237. Kroner, A.; Greenhalgh, A.D.; Zarruk, J.G.; Passos Dos Santos, R.; Gaestel, M.; David, S. TNF and increased intracellular iron alter macrophage polarization to a detrimental M1 phenotype in the injured spinal cord. *Neuron* **2014**, *83*, 1098–1116. [[CrossRef](#)]
238. Rathnasamy, G.; Ling, E.A.; Kaur, C. Iron and iron regulatory proteins in amoeboid microglial cells are linked to oligodendrocyte death in hypoxic neonatal rat periventricular white matter through production of proinflammatory cytokines and reactive oxygen/nitrogen species. *J. Neurosci.* **2011**, *31*, 17982–17995. [[CrossRef](#)]
239. Zhang, Y.; He, M.L. Deferoxamine enhances alternative activation of microglia and inhibits amyloid beta deposits in APP/PS1 mice. *Brain Res.* **2017**, *1677*, 86–92. [[CrossRef](#)]
240. Li, Q.; Wan, J.; Lan, X.; Han, X.; Wang, Z.; Wang, J. Neuroprotection of brain-permeable iron chelator VK-28 against intracerebral hemorrhage in mice. *J. Cereb. Blood Flow Metab.* **2017**, *37*, 3110–3123. [[CrossRef](#)]
241. Mesquita, G.; Silva, T.; Gomes, A.C.; Oliveira, P.F.; Alves, M.G.; Fernandes, R.; Almeida, A.A.; Moreira, A.C.; Gomes, M.S. H-Ferritin is essential for macrophages' capacity to store or detoxify exogenously added iron. *Sci. Rep.* **2020**, *10*, 3061. [[CrossRef](#)]
242. Palmieri, E.M.; Gonzalez-Cotto, M.; Baseler, W.A.; Davies, L.C.; Ghesquiere, B.; Maio, N.; Rice, C.M.; Rouault, T.A.; Cassel, T.; Higashi, R.M.; et al. Nitric oxide orchestrates metabolic rewiring in M1 macrophages by targeting aconitase 2 and pyruvate dehydrogenase. *Nat. Commun.* **2020**, *11*, 698. [[CrossRef](#)] [[PubMed](#)]
243. Court, M.; Petre, G.; Atifi, M.E.; Millet, A. Proteomic Signature Reveals Modulation of Human Macrophage Polarization and Functions Under Differing Environmental Oxygen Conditions. *Mol. Cell. Proteomics.* **2017**, *16*, 2153–2168. [[CrossRef](#)] [[PubMed](#)]
244. Kapralov, A.A.; Yang, Q.; Dar, H.H.; Tyurina, Y.Y.; Anthonymuthu, T.S.; Kim, R.; St Croix, C.M.; Mikulska-Ruminska, K.; Liu, B.; Shrivastava, I.H.; et al. Redox lipid reprogramming commands susceptibility of macrophages and microglia to ferroptotic death. *Nat. Chem. Biol.* **2020**, *16*, 278–290. [[CrossRef](#)] [[PubMed](#)]
245. Ackermann, J.A.; Hofheinz, K.; Zaiss, M.M.; Kronke, G. The double-edged role of 12/15-lipoxygenase during inflammation and immunity. *Biochim. Biophys. Acta Mol. Cell Biol. Lipids* **2017**, *1862*, 371–381. [[CrossRef](#)] [[PubMed](#)]

246. Nnah, I.C.; Lee, C.H.; Wessling-Resnick, M. Iron potentiates microglial interleukin-1beta secretion induced by amyloid-beta. *J. Neurochem.* **2020**, *154*, 177–189. [[CrossRef](#)]
247. Holland, R.; McIntosh, A.L.; Finucane, O.M.; Mela, V.; Rubio-Araiz, A.; Timmons, G.; McCarthy, S.A.; Gun'ko, Y.K.; Lynch, M.A. Inflammatory microglia are glycolytic and iron retentive and typify the microglia in APP/PS1 mice. *Brain Behav. Immun.* **2018**, *68*, 183–196. [[CrossRef](#)]
248. Parrella, E.; Bellucci, A.; Porrini, V.; Benarese, M.; Lanzillotta, A.; Faustini, G.; Longhena, F.; Abate, G.; Uberti, D.; Pizzi, M. NF-kappaB/c-Rel deficiency causes Parkinson's disease-like prodromal symptoms and progressive pathology in mice. *Transl. Neurodegener.* **2019**, *8*, 16. [[CrossRef](#)]
249. Porrini, V.; Mota, M.; Parrella, E.; Bellucci, A.; Benarese, M.; Faggi, L.; Tonin, P.; Spano, P.F.; Pizzi, M. Mild Inflammatory Profile without Gliosis in the c-Rel Deficient Mouse Modeling a Late-Onset Parkinsonism. *Front. Aging Neurosci.* **2017**, *9*, 229. [[CrossRef](#)]
250. Bok, E.; Chung, Y.C.; Kim, K.S.; Baik, H.H.; Shin, W.H.; Jin, B.K. Modulation of M1/M2 polarization by capsaicin contributes to the survival of dopaminergic neurons in the lipopolysaccharide-lesioned substantia nigra in vivo. *Exp. Mol. Med.* **2018**, *50*, 1–14. [[CrossRef](#)]
251. Liu, C.; Zhang, C.W.; Lo, S.Q.; Ang, S.T.; Chew, K.C.M.; Yu, D.; Chai, B.H.; Tan, B.; Tsang, F.; Tai, Y.K.; et al. S-Nitrosylation of Divalent Metal Transporter 1 Enhances Iron Uptake to Mediate Loss of Dopaminergic Neurons and Motoric Deficit. *J. Neurosci.* **2018**, *38*, 8364–8377. [[CrossRef](#)]
252. Chung, K.K.; Thomas, B.; Li, X.; Pletnikova, O.; Troncoso, J.C.; Marsh, L.; Dawson, V.L.; Dawson, T.M. S-nitrosylation of parkin regulates ubiquitination and compromises parkin's protective function. *Science* **2004**, *304*, 1328–1331. [[CrossRef](#)]
253. Roth, J.A.; Singleton, S.; Feng, J.; Garrick, M.; Paradkar, P.N. Parkin regulates metal transport via proteasomal degradation of the 1B isoforms of divalent metal transporter 1. *J. Neurochem.* **2010**, *113*, 454–464. [[CrossRef](#)] [[PubMed](#)]
254. Garrick, M.D.; Zhao, L.; Roth, J.A.; Jiang, H.; Feng, J.; Foot, N.J.; Dalton, H.; Kumar, S.; Garrick, L.M. Isoform specific regulation of divalent metal (ion) transporter (DMT1) by proteasomal degradation. *Biomaterials* **2012**, *25*, 787–793. [[CrossRef](#)] [[PubMed](#)]
255. Zhong, Y.; Li, X.; Du, X.; Bi, M.; Ma, F.; Xie, J.; Jiang, H. The S-nitrosylation of parkin attenuated the ubiquitination of divalent metal transporter 1 in MPP(+)-treated SH-SY5Y cells. *Sci. Rep.* **2020**, *10*, 15542. [[CrossRef](#)] [[PubMed](#)]
256. Zhang, C.W.; Tai, Y.K.; Chai, B.H.; Chew, K.C.M.; Ang, E.T.; Tsang, F.; Tan, B.W.Q.; Hong, E.T.E.; Asad, A.B.A.; Chuang, K.H.; et al. Transgenic Mice Overexpressing the Divalent Metal Transporter 1 Exhibit Iron Accumulation and Enhanced Parkin Expression in the Brain. *Neuromol. Med.* **2017**, *19*, 375–386. [[CrossRef](#)]
257. Paradkar, P.N.; Roth, J.A. Nitric oxide transcriptionally down-regulates specific isoforms of divalent metal transporter (DMT1) via NF-kappaB. *J. Neurochem.* **2006**, *96*, 1768–1777. [[CrossRef](#)] [[PubMed](#)]
258. Boka, G.; Anglade, P.; Wallach, D.; Javoy-Agid, F.; Agid, Y.; Hirsch, E.C. Immunocytochemical analysis of tumor necrosis factor and its receptors in Parkinson's disease. *Neurosci. Lett.* **1994**, *172*, 151–154. [[CrossRef](#)]
259. Hunot, S.; Brugg, B.; Ricard, D.; Michel, P.P.; Muriel, M.P.; Ruberg, M.; Faucheux, B.A.; Agid, Y.; Hirsch, E.C. Nuclear translocation of NF-kappaB is increased in dopaminergic neurons of patients with parkinson disease. *Proc. Natl. Acad. Sci. USA* **1997**, *94*, 7531–7536. [[CrossRef](#)] [[PubMed](#)]
260. Terai, K.; Matsuo, A.; McGeer, P.L. Enhancement of immunoreactivity for NF-kappa B in the hippocampal formation and cerebral cortex of Alzheimer's disease. *Brain Res.* **1996**, *735*, 159–168. [[CrossRef](#)]
261. Zheng, W.; Xin, N.; Chi, Z.H.; Zhao, B.L.; Zhang, J.; Li, J.Y.; Wang, Z.Y. Divalent metal transporter 1 is involved in amyloid precursor protein processing and Abeta generation. *FASEB J.* **2009**, *23*, 4207–4217. [[CrossRef](#)]
262. Ferrari, E.; Capucciati, A.; Prada, I.; Zucca, F.A.; D'Arrigo, G.; Pontiroli, D.; Bridelli, M.G.; Sturini, M.; Bubacco, L.; Monzani, E.; et al. Synthesis, Structure Characterization, and Evaluation in Microglia Cultures of Neuromelanin Analogues Suitable for Modeling Parkinson's Disease. *ACS Chem. Neurosci.* **2017**, *8*, 501–512. [[CrossRef](#)]
263. Hirsch, E.; Graybiel, A.M.; Agid, Y.A. Melanized dopaminergic neurons are differentially susceptible to degeneration in Parkinson's disease. *Nature* **1988**, *334*, 345–348. [[CrossRef](#)] [[PubMed](#)]
264. Walker, D.G.; Lue, L.F.; Beach, T.G.; Tooyama, I. Microglial Phenotyping in Neurodegenerative Disease Brains: Identification of Reactive Microglia with an Antibody to Variant of CD105/Endoglin. *Cells* **2019**, *8*, 766. [[CrossRef](#)]
265. Zecca, L.; Wilms, H.; Geick, S.; Claassen, J.H.; Brandenburg, L.O.; Holzknecht, C.; Panizza, M.L.; Zucca, F.A.; Deuschl, G.; Sievers, J.; et al. Human neuromelanin induces neuroinflammation and neurodegeneration in the rat substantia nigra: Implications for Parkinson's disease. *Acta Neuropathol.* **2008**, *116*, 47–55. [[CrossRef](#)] [[PubMed](#)]
266. Zhang, W.; Zecca, L.; Wilson, B.; Ren, H.W.; Wang, Y.J.; Wang, X.M.; Hong, J.S. Human neuromelanin: An endogenous microglial activator for dopaminergic neuron death. *Front. Biosci.* **2013**, *5*, 1–11. [[CrossRef](#)] [[PubMed](#)]
267. Li, Y.; Pan, K.; Chen, L.; Ning, J.L.; Li, X.; Yang, T.; Terrando, N.; Gu, J.; Tao, G. Deferoxamine regulates neuroinflammation and iron homeostasis in a mouse model of postoperative cognitive dysfunction. *J. Neuroinflamm.* **2016**, *13*, 268. [[CrossRef](#)] [[PubMed](#)]
268. Pan, K.; Li, X.; Chen, Y.; Zhu, D.; Li, Y.; Tao, G.; Zuo, Z. Deferoxamine pre-treatment protects against postoperative cognitive dysfunction of aged rats by depressing microglial activation via ameliorating iron accumulation in hippocampus. *Neuropharmacology* **2016**, *111*, 180–194. [[CrossRef](#)] [[PubMed](#)]
269. Zhang, X.Y.; Cao, J.B.; Zhang, L.M.; Li, Y.F.; Mi, W.D. Deferoxamine attenuates lipopolysaccharide-induced neuroinflammation and memory impairment in mice. *J. Neuroinflamm.* **2015**, *12*, 20. [[CrossRef](#)] [[PubMed](#)]

270. Zhang, W.; Yan, Z.F.; Gao, J.H.; Sun, L.; Huang, X.Y.; Liu, Z.; Yu, S.Y.; Cao, C.J.; Zuo, L.J.; Chen, Z.J.; et al. Role and mechanism of microglial activation in iron-induced selective and progressive dopaminergic neurodegeneration. *Mol. Neurobiol.* **2014**, *49*, 1153–1165. [[CrossRef](#)]
271. Peng, J.; Stevenson, F.F.; Oo, M.L.; Andersen, J.K. Iron-enhanced paraquat-mediated dopaminergic cell death due to increased oxidative stress as a consequence of microglial activation. *Free Radic. Biol. Med.* **2009**, *46*, 312–320. [[CrossRef](#)]
272. Hou, L.; Huang, R.; Sun, F.; Zhang, L.; Wang, Q. NADPH oxidase regulates paraquat and maneb-induced dopaminergic neurodegeneration through ferroptosis. *Toxicology* **2019**, *417*, 64–73. [[CrossRef](#)] [[PubMed](#)]
273. Yauger, Y.J.; Bermudez, S.; Moritz, K.E.; Glaser, E.; Stoica, B.; Byrnes, K.R. Iron accentuated reactive oxygen species release by NADPH oxidase in activated microglia contributes to oxidative stress in vitro. *J. Neuroinflamm.* **2019**, *16*, 41. [[CrossRef](#)] [[PubMed](#)]